



## An improved empirical model for predicting postfire debris-flow volume in the western United States

Alexander N. Gorr<sup>1</sup> ORCID: 0000-0002-3239-7773, Francis K. Rengers<sup>1</sup> ORCID: 0000-0002-1825-0943, Katherine R. Barnhart<sup>1</sup> ORCID: 0000-0001-5682-455X, Matthew A. Thomas<sup>1</sup>  
5 ORCID: 0000-0002-9828-5539, Jason W. Kean<sup>1</sup> ORCID: 0000-0003-3089-0369

<sup>1</sup>U.S. Geological Survey, Geologic Hazards Science Center, Golden, CO, USA

*Correspondence to:* Alexander N. Gorr ([agorr@usgs.gov](mailto:agorr@usgs.gov))

*This draft manuscript is distributed solely for purposes of scientific peer review. Its content is deliberative and pre-decisional, so it must not be disclosed or released by reviewers. Because the manuscript has not yet been approved 10 for publication by the U.S. Geological Survey (USGS), it does not represent any official USGS finding or policy.*

15

20

25



**Abstract.** Accurate estimates of debris-flow volume can be used to help predict the magnitude of runoff-generated postfire debris-flow hazards in the western United States. In this study, we compiled and used a database of 227 postfire debris-flow volumes that were collected across the western United States to develop a multiple linear regression model for predicting postfire debris-flow volume. We explored 36 predictor variables related to rainfall, terrain, and fire characteristics, and selected the model with the combination of variables that yielded the most accurate predictions of debris-flow volume. We evaluated model performance against the entire volume database, as well as against four subsets of volume data from southern California, the Intermountain West, the Southwest, and regions with limited volume data, such as northern California and Washington. We also compared model performance against three existing postfire debris-flow volume models that were developed for use in southern California, the Intermountain West, and the Southwest. We demonstrate that the new volume model performs as well as the regional models in the regions for which they were developed and outperforms existing models when applied to volumes from data-limited regions in the western United States. These results indicate that the debris-flow volume model introduced in this study can be used to improve postfire hazard assessments across the western United States, especially outside of southern California.

## 1 Introduction

Debris flows are a common hazard in mountainous areas around the world (e.g., Rickenmann and Zimmermann, 1993; Wang et al., 2003; Cannon and Gartner, 2005; Sepúlveda et al., 2006; Guthrie et al., 2012; Gartner et al., 2024) but are particularly prevalent in steep landscapes that have been recently burned by wildfire. Wildfire reduces vegetation cover (McGuire et al., 2024a) and alters soil hydraulic properties (e.g., Hoch et al., 2021), which promotes the initiation of runoff-generated debris flows in burned watersheds (e.g., Cannon et al., 2001; Parise and Cannon, 2012; Wall et al., 2020). As a result, burned watersheds are more likely to produce debris flows than comparable unburned watersheds given similar rainfall conditions (McGuire et al., 2021). Burned watersheds also tend to produce larger debris flows than unburned watersheds (Santi and Morandi, 2013), resulting in elevated downstream effects, including the loss of human life (Dowling and Santi, 2014; Kean et al., 2019; Daurio, 2025), damage to infrastructure (e.g., Lancaster et al., 2021), and degradation of water quality (e.g., Smith et al., 2011; Langhans et al., 2016), for communities in fire-prone regions of the western United States (U.S.).

Recent increases in postfire debris-flow activity in the western United States, driven by changes in wildfire activity (Westerling, 2016) and growth in the wildland-urban interface (Radeloff et al., 2018), have motivated the development of a postfire hazard assessment framework that is used by the U.S. Geological Survey (USGS) to mitigate the impact of potential postfire debris flows. The USGS framework uses postfire debris-flow likelihood (Staley et al., 2017) and volume (Gartner et al., 2014) models to generate a combined hazard map for all watersheds within a fire perimeter and identifies the most hazardous watersheds as those that have a high likelihood of debris-flow occurrence and are likely to produce a debris flow that mobilizes a large volume of sediment (Cannon et al., 2010; Landslide Hazards Program, 2018). Methods for predicting debris-flow likelihood can be used to identify which upstream watersheds are likely to produce postfire debris flows. Methods for predicting debris-flow volume, on the other hand, provide insight into the potential magnitude of downstream effects of postfire debris flows, as multiple studies have found that the



area inundated by a debris flow scales with volume (Iverson et al., 1998; Berti and Simoni, 2007; Griswold and Iverson, 2008). Accurate predictions of volume are also used to inform runout models that can evaluate the potential 65 downstream effects of postfire debris flows (Barnhart et al., 2021; Gorr et al., 2022).

Although numerous methods for predicting postfire debris-flow volume have been developed in recent years (e.g., Gartner et al., 2008; Pak and Lee, 2008; Cannon et al., 2010; Santi and Morandi, 2013; Gartner et al., 2014; Pelletier and Orem, 2014; Donovan and Santi, 2017; Wall et al., 2023; Gorr et al., 2024a), none are ideally suited for use in 70 postfire hazard assessment frameworks that are applied across the entire western United States. Multiple volume models have been developed for broad use across the western United States (e.g., Gartner et al., 2008; Cannon et al., 2010; Santi and Morandi, 2013; Pelletier and Orem, 2014) but have deficiencies that limit their use in hazard 75 assessment scenarios. Specifically, existing broadly applicable volume models do not include rainfall variables, despite the fact the volume of postfire debris flows in the western United States is known to scale with short-duration ( $\leq 1$  h) rainfall intensity (Gartner et al., 2008; Pak and Lee, 2008; Cannon et al., 2010; Gartner et al., 2014; Gorr et al., 2024a). The lack of rainfall variables limits the accuracy of these models, particularly when compared to volume 80 models that do include rainfall variables (Gorr et al., 2024a). Volume models that do not consider rainfall are also unable to predict postfire debris-flow volume based on rainfall forecasts, which is a practical benefit offered by volume models that do (Prescott et al., 2024).

There are several postfire debris-flow volume models that include rainfall variables (e.g., Pak and Lee, 2008; Gartner 80 et al., 2008, 2014; Gorr et al., 2024a), but they also have shortcomings that limit their applicability in widespread postfire hazard assessments across the western United States. First, most existing volume models that include rainfall variables are regionally focused to predict volume within a specific area, such as southern California (e.g., Gartner et al., 2014), the Intermountain West (e.g., Wall et al., 2023), or the Southwest (Arizona and New Mexico) (Gorr et al., 2024a). Previous studies have found that these regional models perform well in the areas for which they were 85 developed (e.g., Kean et al., 2019; Wall et al., 2023; Gorr et al., 2024a) but are considerably less accurate when applied to areas outside of their training datasets (e.g., Gorr et al., 2023, 2024a; Rengers et al., 2023, 2024). For example, previous studies have found that a volume model developed for use in southern California (Gartner et al., 2014) overpredicted volumes in other regions of the western United States by up to several orders of magnitude (Gorr et al., 2024a). The decreased performance of regional models in these scenarios may be partially attributed to the fact they 90 use rainfall intensity, even though the intensity of debris-flow-producing rainfall varies widely across the western United States (Staley et al., 2017). As a result, models developed for use in areas where the rainfall intensity required to generate postfire debris flows is low (e.g., Gartner et al., 2014), such as the Transverse Ranges of southern California, where the 15-minute rainfall intensity-duration threshold for debris-flow occurrence is less than 20 mm/h (Staley et al., 2013), tend to overpredict volumes when applied in areas where the intensity required to generate postfire 95 debris flows is much higher, such as northern Arizona, where the 15-minute rainfall intensity-duration threshold for debris-flow occurrence is more than 60 mm/h (Youberg, 2014). Conversely, models developed for use in areas with intense debris-flow-generating rainfall (Gorr et al., 2024a) tend to underpredict volumes in areas with less intense debris-flow-generating rainfall. Furthermore, parts of the western United States lack the volume data needed to



100 develop regional models. For instance, although the Pacific Northwest (Oregon and Washington) and the northern  
Rockies (Idaho, Montana, and Wyoming) are susceptible to postfire debris flows (e.g., Meyer and Wells, 1997; Gabet  
and Bookter, 2008; Wall et al., 2020; Selander et al., 2025), insufficient data has prohibited the development of volume  
models in these regions. The shortcomings of existing postfire debris-flow volume models indicate that a model that  
includes a rainfall variable and can be applied broadly across the western United States would be beneficial for  
improving postfire hazard assessments, particularly in regions with limited volume data.

105 In this study, we developed a new method for predicting postfire debris-flow volume in the western United States for  
the purpose of improving postfire hazard assessments. Specifically, we compiled and used the largest known postfire  
debris-flow volume database with associated rainfall data (Gorr et al., 2025) to develop a multiple linear regression  
model that predicts postfire debris-flow sediment volume. We explored 36 potential predictor variables related to  
rainfall, terrain, and fire characteristics, and selected the combination of three variables that yielded the most accurate  
110 predictions of debris-flow volume. We assessed model performance against the entire volume database, which includes  
227 postfire debris-flow volumes across six states, as well as against three subsets of data from regions in the western  
United States that have published regional volume models: southern California (Gartner et al., 2014), the  
Intermountain West (Wall et al., 2023), and the Southwest (Gorr et al., 2024a). We then compared the performance of  
the new model with three existing regional models. Finally, we evaluated the performance of all four models when  
115 applied to volumes from data-limited regions, which we define as areas that do not have enough volume data to  
develop regional volume models. Results from this study can improve our ability to accurately predict postfire debris-  
flow volume across the western United States, particularly in data-limited regions.

## 2 Data

### 2.1 Debris-flow volumes

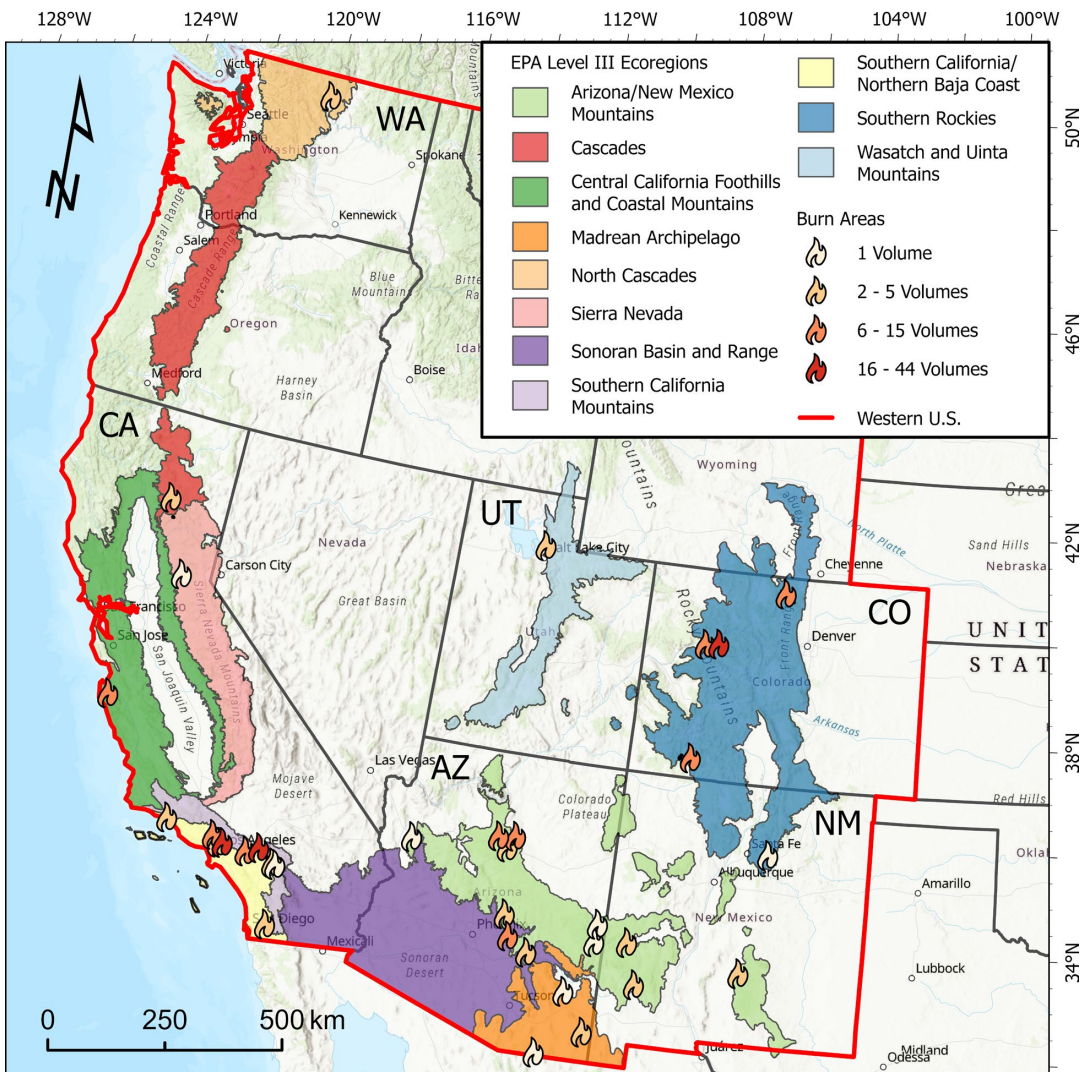
120 We compiled a database of 227 postfire debris-flow volumes from across the western United States (Figure 1) to  
develop the new volume model introduced in this study. Roughly 85% of the database (192 of 227 volumes) consists  
of previously published postfire debris-flow volumes from Arizona (Gorr et al., 2024a); California (Gartner et al.,  
2008; Gartner et al., 2014; Kean et al., 2019; Smith et al., 2021; Swanson et al., 2024), Colorado (Gartner et al., 2008;  
Rengers et al., 2023), New Mexico (Gorr et al., 2024a), and Utah (Gartner et al., 2008). We collected the remaining  
125 15% of volumes (35) from sites in Arizona, northern California, Colorado, New Mexico, and Washington as part of  
this study (Table 1). All volumes represent the volume of sediment deposited downstream from the watershed outlet.  
We did not consider the volume of water mobilized by a flow, nor any sediment that may have been mobilized and  
deposited upstream from the watershed outlet. This is consistent with the data used to develop previous postfire debris-  
flow volume models (e.g., Gartner et al., 2014; Gorr et al., 2024a).

130



**Table 1:** Fire information

Fire Name	Year	State	No. Volume Measurements	Source
Apple	2020	CA	1	Swanson et al. (2024)
Bush	2020	AZ	3	Gorr et al. (2024a)
Buzzard	2018	NM	5	Gorr et al. (2024a)
Cameron Peak	2020	CO	14	Gorr et al. (2025)
Carmel	2020	CA	11	Smith et al. (2021)
Cedar	2003	CA	2	Gartner et al. (2008)
Coal Seam	2002	CO	6	Gartner et al. (2008)
Cub Creek 2	2021	WA	2	Gorr et al. (2025)
Dixie	2021	CA	2	Thomas et al. (2023)
El Dorado	2020	CA	2	Swanson et al. (2024)
Farmington	2003	UT	3	Gartner et al. (2008)
Flag	2021	AZ	1	Gorr et al. (2023)
Frye	2017	AZ	1	Gorr et al. (2024a)
Grand Prix	2003	CA	7	Gartner et al. (2008)
Grizzly Creek	2020	CO	19	Rengers et al. (2024)
Harvard	2005	CA	4	Gartner et al. (2014)
Hermits Peak	2022	NM	1	Gorr et al. (2025)
Horseshoe 2	2011	AZ	4	Gorr et al. (2024a)
Horton	2021	AZ	1	Gorr et al. (2024a)
Missionary Ridge	2002	CO	8	Gartner et al. (2008)
Monument	2011	AZ	1	Gorr et al. (2024a)
Mosquito	2022	CA	1	Gorr et al. (2025)
Museum	2019	AZ	4	Gorr et al. (2024a)
Old	2003	CA	17	Gartner et al. (2008)
Pipeline	2022	AZ	14	Gorr et al. (2025)
Sayre	2008	CA	10	Gartner et al. (2014)
Schultz	2010	AZ	11	Gorr et al. (2024a)
Station	2009	CA	45	Gartner et al. (2014)
Tadpole	2020	NM	4	Gorr et al. (2024a)
Telegraph	2021	AZ	4	Gorr et al. (2024a)
Thomas	2017	CA	5	Kean et al. (2019)
Three Rivers	2021	NM	2	Gorr et al. (2024a)
Wallow	2011	AZ	1	Gorr et al. (2024a)
Woodbury	2019	AZ	11	Gorr et al. (2024a)



135 **Figure 1: Map of the locations of the 34 burn areas included in this study. The burn areas span six states across the western United States (US), including Arizona (AZ), California (CA), Colorado (CO), New Mexico (NM), Utah (UT), and Washington (WA), and 11 Environmental Protection Agency (EPA) Level III Ecoregions. The names of the ecoregions shown in this figure are derived directly from the EPA (U.S. Environmental Protection Agency, 2013). Basemap credits: United States Geological Survey The National Map: 3D Elevation Program,**  
140 **United States Geological Survey Earth Resources Observation & Science Center: GMTED2010.**

The volumes that we compiled were collected using a range of field and remote-sensing techniques. Most volumes were measured using some variation of the field survey methods outlined in Gorr et al. (2024a). In short, measurements of deposit area and average thickness were made in the field and then multiplied to determine debris-flow volume



(e.g., Gorr et al., 2024a; Swanson et al., 2024). Other methods used to measure postfire debris-flow volume in the  
145 field included surveys of closely spaced channel cross-sections (e.g., Gartner et al., 2008) and counting the number of trucks filled with sediment when emptying a debris-retention basin (truck counts) (Gartner et al., 2014). The remaining volumes were measured primarily using remote-sensing techniques. Most commonly, these volumes were calculated using digital elevation models (DEM) of difference (DoD) that were generated by differencing pre-event and post-event light detection and ranging (lidar) (Smith et al., 2021; Rengers et al., 2024; Swanson et al., 2024). In other cases, 150 high-resolution aerial imagery was used to help constrain the area of larger debris flows, and volume was calculated by multiplying the area by depth measurements made in the field (e.g., Gorr et al., 2024a).

Variations in the size of the debris-flow volumes included in this database, and the techniques used to measure them, mean that the uncertainty associated with each volume varies widely. Santi (2014) determined that the uncertainty associated with deposit boundary and thickness measurements, the most used method to measure volumes in this  
155 database, was -25% to +35% for small debris flows ( $\sim 1,500 \text{ m}^3$ ), -28% to +30% for medium debris flows ( $\sim 15,000 \text{ m}^3$ ), and -9% to +17% for large debris flows ( $\sim 150,000 \text{ m}^3$ ). Other field measurement techniques, such as truck counts and channel cross-section surveys, have a lower degree of uncertainty, but still vary between -25% and +20%, depending on debris-flow size (Santi, 2014). The uncertainty associated with volumes measured by remote sensing techniques are less constrained, but we estimate that the volumes calculated by lidar differencing have an uncertainty  
160 of -14% to +14%, based on a  $\pm 10 \text{ cm}$  level of detection (LoD) (Rengers et al., 2024). Overall, given the wide range of debris-flow sizes and measurement techniques included in the volume database, we conservatively estimate the uncertainty associated with these volume measurements to be  $\pm 25\%$ .

The volume database includes data from 195 watersheds from 34 burn areas across six states in the western United  
165 States, a region we define as the states of Arizona, California, Colorado, Idaho, Montana, Nevada, New Mexico, Oregon, Utah, Washington, and Wyoming (Figure 1; Table S1). Specifically, the volume database includes volumes from Arizona, California, Colorado, New Mexico, Utah, and Washington (Figure 1). The burn areas included in this study range in size from  $4.2 \text{ km}^2$  to  $3,965 \text{ km}^2$  and span a wide range of climatological settings. The mean annual precipitation at the burn areas ranges from 396 mm to 1,343 mm, and the mean annual temperature ranges from 3.7  $^{\circ}\text{C}$  to 17.8  $^{\circ}\text{C}$  (PRISM Climate Group, 2025) (Table S1).

170 The burn areas are also geographically and ecologically diverse, as they span 11 Level III ecoregions, or areas where ecosystems and ecosystem components, including geology, vegetation, climate, and hydrology, are generally similar (U.S. Environmental Protection Agency, 2013) (Figure 1). The names of the ecoregions presented here are derived directly from U.S. Environmental Protection Agency (2013). The Arizona/New Mexico Mountains ecoregion, which is characterized by steep foothills, mountains, and dissected plateaus (Wilken et al., 2011), contains 12 burn areas.  
175 Grassland, chaparral, and pinyon-juniper and oak woodlands grow at lower elevations in this ecoregion, whereas ponderosa pine and mixed-conifer forests are common at higher elevations (Wilken et al., 2011). The Southern California Mountains ecoregion contains seven burn areas (Figure 1). This ecoregion contains the high-elevation Transverse Ranges, which serve as a buffer between a coastal Mediterranean climate to the west and a dry, desert climate to the east. Chapparal and oak woodlands are the predominant vegetation communities in this region, although



180 coniferous forests are found at higher elevations (Griffith et al., 2016). The Southern Rockies ecoregion, which includes most of western Colorado, as well as parts of southern Wyoming and northern New Mexico, contains an additional five burn areas (Figure 1). It consists primarily of steep, high-elevation mountain ranges, with some intermontane valleys, and the dominant vegetation communities vary based on a steep elevation gradient. Grasslands and shrublands are common at lower elevations, ponderosa pine, aspen, juniper, and oak forests at middle elevations, 185 mixed-conifer forests at higher elevations, and alpine vegetation at the highest elevations (Wilken et al., 2011; Drummond, 2012). The remaining 12 burn areas are spread across an additional eight ecoregions that contain between one to three burn areas each (Figure 1). These ecoregions range from the high, rugged mountains and dense coniferous forests of the North Cascades ecoregion to the low, broad basins and microphyllous scrubland of the Sonoran Basin and Range ecoregion (Wilken et al., 2011).

190 **2.2 Rainfall, topography, and fire severity data**

In addition to debris-flow volume data, we also collected data related to rainfall, terrain, and fire characteristics to calculate 36 potential predictor variables for use in the development of the new volume model, as described in more detail in Section 3.1. We collected rainfall data for every debris-flow-producing storm using a series of rain gages located near watersheds with volume measurements. The rain gages we used were installed and maintained by local, 195 state, and federal government agencies including, but not limited to, the Los Angeles County Department of Public Works (Gartner et al., 2014), Arizona Department of Water Resources (Gorr et al., 2024a), U.S. Forest Service (Gorr et al., 2024a), and the USGS (Gartner et al., 2014), as well as universities (Smith et al., 2021), and private consulting firms (Gorr et al., 2024a). To ensure that the recorded rainfall was representative of the debris-flow-producing storms, we used rain gages located within 4 km of watersheds with debris-flow volume measurements as suggested by Staley 200 et al. (2017). Most rain gages, however, were located within 2 km of the debris-flow-producing watersheds. We could attribute most debris-flow volumes to a single storm, but when there were multiple storms prior to a volume measurement, we followed the methods of Gartner et al. (2014) and attributed the volume to the most intense storm that occurred between the assumed debris-flow initiation date and the volume measurement. We defined individual storms as events that were separated by at least eight hours without rainfall (Staley et al., 2020).

205 We used national datasets to calculate metrics related to terrain and fire characteristics for each debris-flow-producing watershed included in our database. Specifically, we resampled the 1/3 arc-second seamless DEM dataset from the USGS 3D Elevation Program (3DEP) to create a series of 10-m resolution DEMs that we used to delineate watershed boundaries and calculate terrain metrics for each watershed. We manually defined the outlet of each watershed as the point immediately upstream from the debris-flow deposit used to calculate volume, ensuring that all terrain metrics 210 only considered the watershed area that contributed to debris-flow volume. This also ensured consistency among metrics related to fire characteristics, which we calculated using data from the Monitoring Trends in Burn Severity (MTBS) program (Monitoring Trends in Burn Severity, 2025). MTBS provides information for all fires 1,000 acres and larger in the western United States that burned from 1984 to present, including ignition date, fire severity, and differenced Normalized Burn Ratio (dNBR) data (Monitoring Trends in Burn Severity, 2025). The differenced



215 Normalized Burn Ratio is a remote sensing index that measures fire-induced changes in vegetation by comparing pre-  
and post-fire satellite imagery and is commonly used to classify burn severity (Parsons et al., 2010).

### 3 Methods

#### 3.1 Calculation of predictor variables

220 We calculated 36 potential predictor variables for use in model development: six rainfall variables, 13 terrain variables,  
and 17 variables related to fire characteristics. We analyzed six variables related to peak rainfall intensity and rainfall  
ratios (Table 2) because previous work indicates that hourly or sub-hourly rainfall intensity data can be used to more  
accurately constrain postfire debris-flow volume (e.g., Pak and Lee, 2008; Gartner et al., 2014; Gorr et al., 2024a).  
225 We define a rainfall ratio as a recorded rainfall metric normalized by that same metric associated with a 1-year  
recurrence interval storm at a given location (Cavagnaro et al., 2025a). For example, we define the rainfall ratio of the  
peak rainfall intensity measured over a 15-minute duration ( $i_{15}$ ) as the recorded  $i_{15}$  normalized by the  $i_{15}$  associated  
with a 1-year recurrence interval storm at a given watershed. Similarly, we define the rainfall ratios of the peak rainfall  
intensity measured over 30-minute ( $i_{30}$ ) and 60-minute ( $i_{60}$ ) durations as the recorded  $i_{30}$  or  $i_{60}$  normalized by the  
 $i_{30}$  or  $i_{60}$  associated with a 1-year recurrence interval storm at a given watershed.

**Table 2:** Summary statistics for rainfall predictor variables, as well as the transformation of each variable (e.g., no transformation (None) or natural log (Ln)) that yielded the most linear relationship with debris-flow volume, which we determined using the Pearson product-moment correlation coefficient ( $\rho$ ).

Predictor Variable	Min.	Max.	Mean	Median	Transform	$\rho$
Peak 15-minute rainfall intensity ( $i_{15}$ ) (mm/h)	5	124	49	37	None	-0.11
Peak 30-minute rainfall intensity ( $i_{30}$ ) (mm/h)	4	82	34	26	None	-0.13
Peak 60-minute rainfall intensity ( $i_{60}$ ) (mm/h)	2	51	22	21	None	-0.13
$i_{15}$ Rainfall ratio	0.16	2.96	1.36	1.21	Ln	0.04
$i_{30}$ Rainfall ratio	0.14	3.19	1.39	1.32	None	-0.03
$i_{60}$ Rainfall ratio	0.13	3.00	1.37	1.27	None	-0.09

230 We selected a 1-year recurrence interval to calculate rainfall ratio, as postfire debris-flows in the western United States  
are generated by storms with a 1-year recurrence interval, on average (Staley et al., 2020). When available, we used  
National Oceanic and Atmospheric Administration (NOAA) Atlas 14 precipitation frequency data (Bonnin et al., 2006;  
Perica et al., 2013, 2014) to determine the  $i_{15}$ ,  $i_{30}$ , and  $i_{60}$  of 1-year recurrence interval storms at each debris-flow-  
producing watershed. For one burn area where Atlas 14 data were not available (Cub Creek 2), we used NOAA Atlas  
235 2 data (Miller et al., 1973) to estimate the  $i_{15}$ ,  $i_{30}$ , and  $i_{60}$  of a 1-year recurrence interval storm. When known, we  
determined the 1-year recurrence interval values at the location of the rain gage where rainfall was recorded. If we did  
not know the location of the rain gage (i.e., the coordinates of the gage were not provided by a previous study), we  
used the 1-year recurrence interval rainfall associated with the centroid of the associated watershed. We considered  
rainfall ratio metrics because previous studies have identified a relationship between postfire debris-flow likelihood



240 and rainfall ratio (referred to as “rainfall anomaly” in Cavagnaro et al., 2025a), suggesting that there may also be a relationship with postfire debris-flow volume.

**Table 3:** Summary statistics for watershed terrain predictor variables, as well as the transformation of each variable (e.g., natural log (Ln) or square root ( $\sqrt{\cdot}$ )) that yielded the most linear relationship with debris-flow volume, which we determined using the Pearson product-moment correlation coefficient ( $\rho$ ).

Predictor Variable	Min.	Max.	Mean	Median	Transform	$\rho$
Watershed area (km <sup>2</sup> )	0.01	28.0	1.55	0.41	Ln	0.79
Relief (m)	88	2,031	538	481	$\sqrt{\cdot}$	0.72
Mean elevation (m) <sup>a</sup>	253	3,000	1,626	1,377	Ln	0.05
Mean slope (°) <sup>a</sup>	11.1	50.6	30.1	29.7	Ln	0.05
Area with slopes $\geq 23^\circ$ (km <sup>2</sup> )	0.00	24.7	1.02	0.29	$\sqrt{\cdot}$	0.74
Mean slope (%) <sup>a</sup>	19.7	155.5	60.5	60.4	Ln	0.03
Area with slopes $\geq 30\%$ (km <sup>2</sup> )	0.00	26.1	1.21	0.34	$\sqrt{\cdot}$	0.74
Area with slopes $\geq 50\%$ (km <sup>2</sup> )	0.00	23.4	0.89	0.26	$\sqrt{\cdot}$	0.74
Maximum flow path (m)	217	10,669	1,945	1,456	Ln	0.74
Total channel length (m)	22	189,451	10,160	2,400	$\sqrt{\cdot}$	0.69
Drainage density (km <sup>-1</sup> ) <sup>a</sup>	1.37	12.6	6.32	6.20	$\sqrt{\cdot}$	0.10
Relief ratio	0.11	1.76	0.36	0.32	Ln	-0.50
Ruggedness	0.20	2.86	0.80	0.66	Ln	-0.58

<sup>a</sup>Variable removed because it was not linearly related to volume

245 We also calculated 13 terrain variables that previous studies found were correlated with postfire debris-flow volume (Gartner et al., 2014; Wall et al., 2023; Gorr et al., 2024a) for all 195 debris-flow-producing watersheds using ArcGIS Pro 3.3.0 (Table 3). Here we define relief (Table 3) as the difference between the maximum elevation and minimum elevation within a watershed, maximum flow path as the longest flow path within a watershed, as measured from the watershed outlet to the top of the drainage divide, and total channel length as the combined length of all channels within a watershed. Drainage density is defined as the total channel length divided by the watershed area, relief ratio as the length of the maximum flow path divided by watershed relief, and ruggedness, also known as the Melton ratio, 250 as watershed relief divided by the square root of watershed area. We used 10-m DEMs to calculate these variables because this was the highest resolution data available for every watershed. Ensuring consistency across sites was necessary, as several of the terrain variables that we calculated (e.g., slope) were dependent on DEM resolution (Smith et al., 2019).



**Table 4:** Summary statistics for fire predictor variables, as well as the transformation of each variable (e.g., natural log (Ln) or square root ( $\sqrt{\cdot}$ )) that yielded the most linear relationship with debris-flow volume, which we determined using the Pearson product-moment correlation coefficient ( $\rho$ ).

Predictor Variable	Min.	Max.	Mean	Median	Transform	$\rho$
Time since fire (yrs) <sup>a</sup>	0.04	3.17	0.48	0.25	Ln	-0.18
Area burned (km <sup>2</sup> )	0.00	23.3	1.36	0.38	$\sqrt{\cdot}$	0.72
Area burned at low severity (km <sup>2</sup> )	0.00	4.82	0.33	0.08	$\sqrt{\cdot}$	0.61
Area burned at moderate severity (km <sup>2</sup> )	0.00	17.7	0.82	0.19	$\sqrt{\cdot}$	0.72
Area burned at high severity (km <sup>2</sup> )	0.00	2.48	0.21	0.02	$\sqrt{\cdot}$	0.46
Area burned at mod/high severity (km <sup>2</sup> )	0.00	18.5	1.03	0.26	$\sqrt{\cdot}$	0.72
Area burned with slopes $\geq 23^\circ$ (km <sup>2</sup> )	0.00	20.3	0.92	0.28	$\sqrt{\cdot}$	0.73
Area burned mod/high with slopes $\geq 23^\circ$ (km <sup>2</sup> )	0.00	15.8	0.71	0.17	$\sqrt{\cdot}$	0.74
Area burned with slopes $\geq 30\%$ (km <sup>2</sup> )	0.00	21.6	1.09	0.31	$\sqrt{\cdot}$	0.74
Area burned mod/high with slopes $\geq 30\%$ (km <sup>2</sup> )	0.00	17.0	0.84	0.21	$\sqrt{\cdot}$	0.73
Area burned with slopes $\geq 50\%$ (km <sup>2</sup> )	0.00	19.1	0.79	0.24	$\sqrt{\cdot}$	0.73
Area burned mod/high with slopes $\geq 50\%$ (km <sup>2</sup> )	0.00	14.8	0.61	0.14	$\sqrt{\cdot}$	0.74
2 x area burned mod/high + 1 x area low (km <sup>2</sup> )	0.00	41.8	2.39	0.68	$\sqrt{\cdot}$	0.72
4 x area burned mod/high + 1 x area low (km <sup>2</sup> )	0.00	78.9	4.44	1.18	$\sqrt{\cdot}$	0.72
Fraction of watershed burned <sup>a</sup>	0.03	1.00	0.90	0.98	Ln	0.11
Fraction of watershed burned mod/high <sup>a</sup>	0.00	1.00	0.68	0.74	$\sqrt{\cdot}$	0.21
Mean differenced Normalized Burn Ratio <sup>a</sup>	6	842	353	340	Ln	0.17

<sup>a</sup>Variable removed because it was not linearly related to volume

255

We calculated another 17 variables related to fire characteristics (Table 4) that previous studies have found to be correlated with postfire debris-flow volume using data from MTBS (Gartner et al., 2014; Wall et al., 2023; Gorr et al., 2024a). We define time since fire (Table 4) as the time between the date of fire ignition and the date of debris-flow initiation. Mean dNBR is the only fire variable that we considered that has not been explored by previous volume 260 studies (e.g., Gartner et al., 2014; Wall et al., 2023; Gorr et al., 2024a). We included it in this analysis because it has been identified as an important control on postfire debris-flow likelihood (Staley et al., 2017), and because it provides an objective measure of how severely a watershed has been affected by fire.

### 3.2 Model development

#### 3.2.1 Initial screening of predictor variables

265 After identifying 36 potential predictor variables related to rainfall (Table 2), watershed terrain (Table 3), and fire characteristics (Table 4), we used a multiple linear regression analysis to develop a model for predicting postfire



debris-flow volume in the western United States. Multiple linear regression is a statistical technique that uses multiple predictor variables to estimate the value of a response variable (debris-flow volume) following the general form:

$$y = \beta_0 + \beta_1 x_1 + \beta_2 x_2 + \dots + \beta_k x_k + \varepsilon \quad (1)$$

270 where  $y$  is the response variable,  $\beta_0$  is the intercept,  $x_i$  is the  $i$ th predictor variable,  $\beta_i$  is the slope coefficient for the  $i$ th predictor variable,  $x_k$  and  $\beta_k$  and are the  $k$ th predictor variable and the slope coefficient for the  $k$ th predictor variable, respectively, and  $\varepsilon$  is the error term.

275 We started the model development process by ensuring that each potential predictor variable was linearly related to debris-flow volume, as a linear relationship between predictor variable and response variable is a requirement of multiple linear regression (Helsel et al., 2020). First, we used the Pearson product-moment correlation coefficient ( $\rho$ ) to quantify the relationship between the response variable and each predictor variable. We then took the square root and natural log of the response and predictor variables to assess whether transforming one, or both, variables resulted in a more linear relationship between the two. This process resulted in nine correlation coefficients, representing the relations between the response variable and the predictor variable after applying each of three transformations (no 280 transform, square root, and natural log) to both variables. Using this information, we selected the transformations that yielded the highest value of  $\rho$ , and thus the most linear relationship between the variables (Tables 2-4). Additionally, because  $\rho$  can be heavily influenced by outliers or a curved relationship between response and predictor variables (Helsel et al., 2020), we used scatter plots to visually confirm that debris-flow volume and each predictor variable exhibited a linear relationship. Using these plots, we determined that predictor variables that had a  $\rho$  value between - 285 0.3 and 0.3 did not exhibit a convincing linear relationship with debris-flow volume. As a result, we removed these variables from our analysis (Tables 3 and 4).

290 We made an exception to the requirement that each predictor variable be linearly related to debris-flow volume for variables related to rainfall. Although none of the rainfall variables explored here had a correlation coefficient stronger than  $\pm 0.3$  (Table 2), we did not remove them from our analysis, as previous studies have found that including a rainfall 295 variable can result in more accurate estimates of postfire debris-flow volume (e.g., Pak and Lee, 2008; Gartner et al., 2014; Gorr et al., 2024a). For instance, Gorr et al. (2024a) found that volume models that contained a rainfall variable considerably outperformed those that did not, despite a weak relationship between the rainfall variables they considered and debris-flow volume. We attribute the weak relationship between rainfall variables and debris-flow volume in this study to uncertainty in the rainfall data. Though we only used data from rain gages within 4 km of debris-flow-producing watersheds, spatial variations in rainfall may have still resulted in substantial differences 300 between what was measured by a rain gage and actual rainfall conditions in the watershed (Figure S1). This situation was likely more common in states like Arizona, Colorado, and New Mexico, where most debris flows initiate as the result of highly localized convective storms (e.g., Cannon et al., 2008; Gorr et al., 2023; McGuire et al., 2024b). However, this uncertainty and lack of linearity is in line with that of rainfall data used in previous volume studies (e.g., Gartner et al., 2014; Gorr et al., 2024a), so we did not remove any rainfall variables from our analysis based on the linear relationship requirement. As a result, we were left with 28 potential predictor variables for model development.



### 3.2.2 Predictor variable selection and model calibration

We selected the predictor variables for the new volume model using a multi-step procedure designed to maximize model performance, minimize the number of predictor variables used, and ensure that the final model met all requirements for multiple linear regression. Because we considered 28 predictor variables, there were  $2^{28}$  potential variable combinations that we could have evaluated. Instead of considering all  $2^{28}$  potential variable combinations, we grouped the variables into three bins (rainfall, terrain, and fire) and only considered models that contained one variable from each bin (n=702). Following the methods outlined below, we fit each of the 702 models, selected those that met the requirements of multiple linear regression (i.e., had residuals that were normally distributed and had a constant variance) (Helsel et al., 2020), identified a subset of similarly performing top models (n=29), and made final variable selection based on additional multiple linear regression requirements and the relative frequency of occurrence of predictor variables within the top model subset.

We started the variable selection process by separating each of the remaining 28 predictor variables into three bins (six rainfall variables, nine terrain variables, and 13 fire variables) and only considered models that selected one variable from each bin to prevent multicollinearity. Multicollinearity occurs when one predictor variable is closely related to another, and it can result in unrealistically large slope coefficients and illogical relationships between predictor and response variables (Eq. 1), negatively impacting model performance (Alin, 2010; Helsel et al., 2020). Separating the predictor variables into bins reduced the likelihood of selecting two variables that exhibited multicollinearity (e.g., watershed area with slopes  $\geq 23^\circ$  and watershed area with slopes  $\geq 30\%$ ). This process yielded 702 unique combinations of rainfall, terrain, and fire predictor variables. We then fit a multiple linear regression model to each combination, resulting in 702 unique, three-variable models.

After independently fitting all 702 models, we evaluated each to ensure they met the following requirements of multiple linear regression: that the residuals were normally distributed and that the residuals had a constant variance (Helsel et al., 2020). These requirements ensure valid hypothesis tests and reliable confidence and prediction intervals for the model (Helsel et al., 2020). We used the Anderson-Darling (AD) test (Anderson and Darling, 1954) to assess the normality of model residuals, and the Brown-Forsythe (BF) test (Brown and Forsythe, 1974) to assess the variance of the residuals. The null hypothesis for the AD test is that the residuals follow a normal distribution. Therefore, an AD p-value  $>0.05$  indicates that the null hypothesis cannot be rejected and that the residuals are normally distributed. The null hypothesis for the BF test is that the residuals have a constant variance, so a BF p-value  $>0.05$  means that the null hypothesis cannot be rejected and that there is a constant variance in the residuals. To ensure our final model met these requirements of multiple linear regression, we removed 570 models that did not pass the AD and/or BF tests from consideration, leaving 132 models for further analysis.

After removing the models that did not fit our statistical requirements, we evaluated the performance of the remaining 132 models against the entire volume database using metrics including  $R^2$  and root mean square error (RMSE). Higher  $R^2$  values and lower RMSE values reflected better model performance. We also calculated the percentage of volumes predicted within an order of magnitude by each model, as having a first order estimate of debris-flow magnitude is useful for rapid hazard assessment scenarios. We used these metrics to further reduce the number of models we



considered during our final model selection process by removing all models where the  $R^2$  and RMSE values were not within 10% of those of the best-performing model. This resulted in 29 models to consider for final evaluation.

340 From the remaining 29 models, we selected one final model using several factors in addition to the metrics outlined above. First, we determined how often each rainfall, terrain, and fire variable appeared in the 29 best-performing models, and prioritized models that used more commonly selected variables. Given the similar quantitative performance of the remaining 29 models, we interpreted variables that appeared more frequently as those that were more important for constraining postfire debris-flow volume using our dataset. We also ensured that there was no  
345 multicollinearity between the selected predictor variables for each model using the variance inflation factor (VIF) (Marquardt, 1970). We interpreted VIF values over 10 as indicative of a strong relationship between predictor variables (Helsel et al., 2020). We used a p-value of 0.1 to assess whether the predictor variables included in each model were statistically significant and removed any models that contained one or more predictor variables with a p-value  $> 0.1$  from consideration. Finally, we assessed whether the predictor variables included in each model fit our conceptual  
350 understanding of postfire debris-flow growth. For example, it is well-established that more intense rainfall tends to produce larger debris-flow volumes (e.g., Gartner et al., 2014; Gorr et al., 2024a), so we did not consider models that exhibited a negative relationship between rainfall intensity and volume. Using these considerations, in addition to the quantitative performance metrics, we selected a final model for predicting postfire debris-flow volume in the western United States, which we refer to hereafter as the western United States (WEST) model.

355 **3.3 Model validation**

We ensured the WEST model was not overfit using iterated fivefold cross validation (Kohavi, 1995), a method that has been used to validate previous postfire debris-flow volume models (e.g., Gorr et al., 2024a). We started this process by randomly separating the volume database into five similarly sized groups, four of which we classified as the training dataset and one as the testing dataset. We then fit the model on the training dataset and evaluated its performance  
360 against the testing dataset using  $R^2$  and RMSE. We repeated this process four more times so that each group of volumes was used as part of the training dataset four times and as the testing dataset once, resulting in five  $R^2$  and RMSE values that we averaged to determine a mean  $R^2$  and RMSE for that iteration of the fivefold cross validation. Then, we started the entire process over again by randomly splitting the volume database into five new groups. In total, we completed 20 iterations of fivefold cross validation to more robustly evaluate the model's performance when applied to different  
365 subsets of data. This process yielded 100 distinct groups of volume data that were used for both training and testing, as well as 20 averaged  $R^2$  and RMSE values. We once again averaged the mean  $R^2$  and RMSE values to determine a single cross-validated (CV)  $R^2$  and RMSE, which we used to evaluate how well the model performed against unseen data. We also assessed the distribution of the  $R^2$  and RMSE values associated with all 100 folds to determine how generalizable the model was to different subsets of volume data. We interpreted CV  $R^2$  and RMSE values similar to  
370 the  $R^2$  and RMSE of the WEST model trained on the entire dataset as an indication that the model was not overfit, and a narrow range of  $R^2$  and RMSE values as an indication that the model was not overly sensitive to volumes from specific geographic regions.

**3.4 Comparison with existing models**



We compared the performance of the WEST model against the performance of three existing postfire debris-flow volume models: the Emergency Assessment volume (EAV) model (Gartner et al., 2014), the Intermountain West (IMW) volume model (Wall et al., 2023), and the V1 volume model (Gorr et al., 2024a). Although other methods for predicting postfire debris-flow volume exist (Santi and Morandi, 2013; Pelletier and Orem, 2014; Donovan and Santi, 2017), we selected the EAV, IMW, and V1 models, in particular, for comparison because they were developed for the purpose of postfire hazard assessment using at least in part, subsets of volume data from the larger volume database used in this study (Gartner et al., 2014; Wall et al., 2023; Gorr et al., 2024a). However, unlike the WEST model, which was developed using data from across the western United States (Figure 1), these models were developed using data from more specific geographic regions, including southern California (Gartner et al., 2014), the Intermountain West, defined as the states of Arizona, Colorado, Idaho, Montana, Nevada, New Mexico, Utah, and Wyoming (Wall et al., 2023), and the Southwest, defined as the states of Arizona and New Mexico (Gorr et al., 2024a). Note that the Southwest is a smaller region within the larger Intermountain West, and both regions include the states of Arizona and New Mexico. The IMW model was developed for a broad region that includes Arizona and New Mexico (Wall et al., 2023), whereas the V1 model was developed for use in Arizona and New Mexico, specifically (Gorr et al., 2024a). We compared the WEST model to these three regional models to further evaluate model performance against existing methods for constraining postfire debris-flow volume.

We evaluated and compared the performance of each of the models when applied to the entire western United States database. Additionally, to more fairly compare the existing models to the WEST model, we also evaluated the performance of each model when applied to subsets of data from the regions for which the existing models were developed: southern California (Gartner et al., 2014), the Intermountain West (Wall et al., 2023), and the Southwest (Gorr et al., 2024a). The southern California dataset consisted of 93 debris-flow volumes from the Transverse Ranges (Table 1), the Intermountain West dataset of 118 volumes from the states of Arizona, Colorado, New Mexico, and Utah, and the Southwest dataset of 68 volumes from Arizona and New Mexico (Table 1). By assessing the performance of each model against these subsets of volume data, we were able to evaluate how the WEST model performed against regional models when applied to the regions in which those models were developed. We also evaluated how each of the models performed against volumes from data-limited regions, which we define as regions where there is currently not enough volume data to develop a regional volume model. The data-limited dataset included 19 total volumes: 14 from northern California, 3 from Utah, and 2 from Washington (Table S2).

We used multiple metrics to evaluate the performance of each model across the five subsets of volume data. We visually assessed the goodness of fit of each model by plotting the probability density function of model residuals and quantified it by calculating the mean ( $\mu$ ) and standard deviation ( $\sigma$ ) of the residuals. Residual mean values closer to zero and smaller  $\sigma$  values indicate better model performance. We also calculated the median absolute error (MAE) and the percentage of volumes predicted within an order of magnitude to further assess model performance. Because all four volume models were developed in natural logarithmic space (Gartner et al., 2014; Wall et al., 2023; Gorr et al., 2024a), we present  $\mu$  and  $\sigma$  values in their natural log transformed form. However, we present the MAE and percentage of volumes predicted within an order of magnitude in dimensional space for better interpretability.



410 4 Results

#### 4.1 WEST model

Using the methods outlined in Section 3.2, we selected one model for predicting postfire debris-flow volume in the western United States. The WEST model predicts the volume of sediment deposited by postfire debris flows using the equation:

415 
$$\ln V = 7.56 + 0.20i_{30rr} + 0.75 \ln a + 1.11\sqrt{mh_{50}} \quad (2)$$

where  $V$  is debris-flow volume ( $\text{m}^3$ ),  $i_{30rr}$  is the  $i30$  rainfall ratio,  $a$  is watershed area ( $\text{km}^2$ ), and  $mh_{50}$  is watershed area burned at moderate or high severity with slopes  $\geq 50\%$  ( $\sim 27^\circ$ ) ( $\text{km}^2$ ). The WEST model had an  $R^2 = 0.66$  and a RMSE = 1.31, both of which were the best among the 29 final models discussed in Section 3.2.2 (Tables S3 and S4). The VIF for each predictor variable in the WEST model was less than three, indicating that there was no 420 multicollinearity, and the p-value for all three predictor variables was  $< 0.1$ , indicating that each was statistically significant.

The WEST model overpredicted 48% of volumes in the database and underpredicted the remaining 52% (Figure 2). It predicted 41% of volumes within  $1,000 \text{ m}^3$ , 75% within  $10,000 \text{ m}^3$ , and 98% within  $100,000 \text{ m}^3$  of what was observed. It also predicted 93% of volumes within an order of magnitude (Figure 2). Additionally, the relations among 425 debris-flow volume and each of the predictor variables selected for inclusion in the WEST model agreed with our conceptual understanding of postfire debris-flow growth, as more intense rainfall, larger watersheds, steeper slopes, and higher burn severity yielded greater sediment volumes (Eq. 2).

Results of the cross-validation (CV) evaluation indicated that the WEST model was not overfit and was not overly sensitive to volumes from any particular geographic region (Figure S2). The CV  $R^2$  and RMSE values were 0.63 and 430 1.32, respectively, closely matching the  $R^2$  (0.66) and RMSE (1.31) values of the WEST model trained on the entire volume database. This demonstrated that the model generalized well to unseen data. Additionally, the distributions of the 100 fold-level  $R^2$  and RMSE were relatively narrow (Figure S2), with standard deviations of 0.08 and 0.13, respectively, indicating that, although there was some fold-to-fold variability, most splits produced broadly similar 435 performance, regardless of the geographic distributions of the volumes. Furthermore, the 20 mean  $R^2$  and RMSE values (one associated with each iteration of fivefold cross validation) varied only slightly (Figure S2), providing additional evidence that model performance was stable across random splits of the volume database.

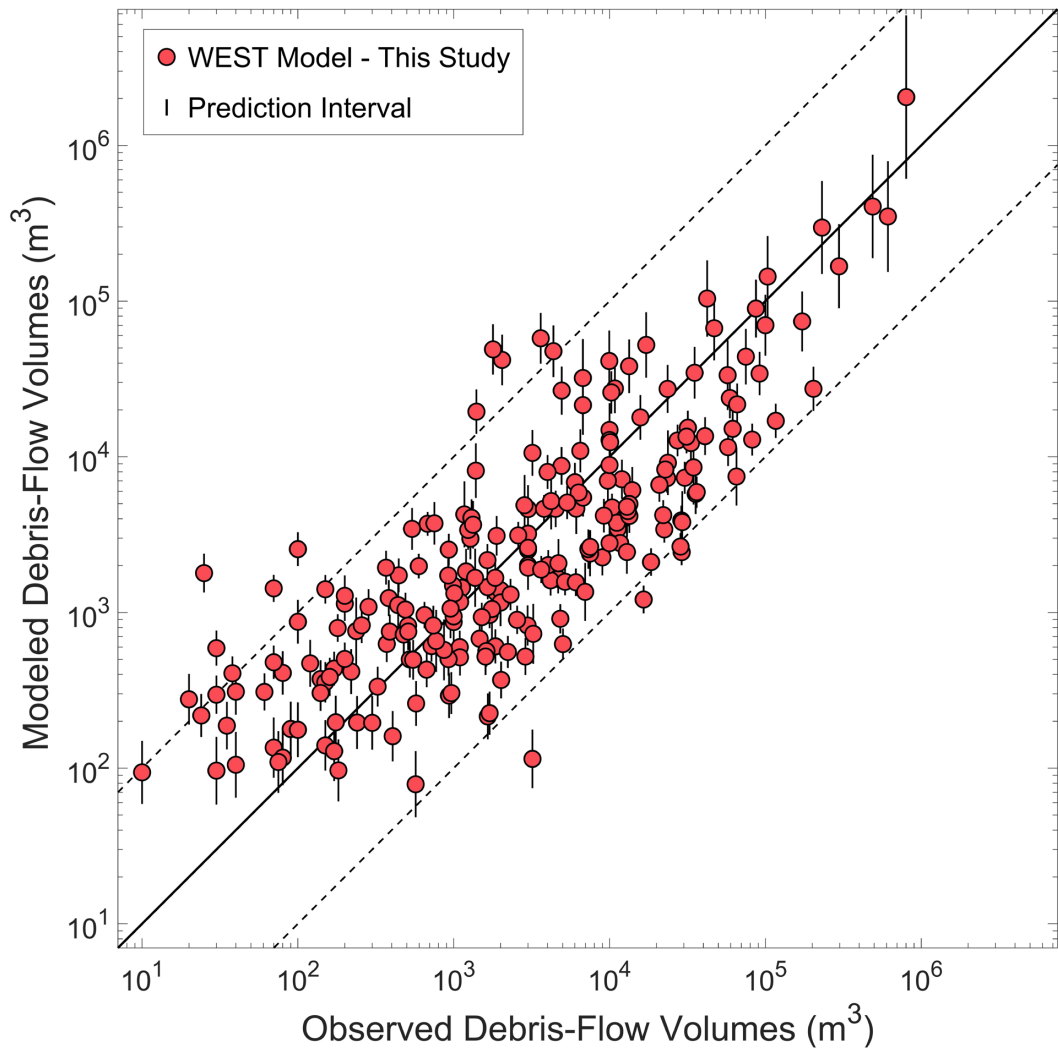


Figure 2: A comparison between the observed volume of all 227 postfire debris flows and the corresponding volume predicted by the Western United States (WEST) model. Vertical lines represent the 95% prediction interval associated with each point. The thick, black line is a 1:1 line, and the thin, dashed lines represent an order of magnitude envelope.

#### 4.2 Comparison with existing models

The WEST model outperformed the EAV (Gartner et al., 2014), IMW (Wall et al., 2023), and V1 (Gorr et al., 2024a) models when applied to the entire western United States volume database. Probability density functions of model residuals revealed that the WEST model provided the best fit between observed and modeled postfire debris-flow volumes in the western United States (Figure 3). The WEST model had a residual mean ( $\mu$ ) nearly equal to zero (Table

445



5), indicating that it did not systemically overpredict or underpredict debris-flow volumes in the western United States (Figure 3a). In contrast, the EAV model (Figure 3b) had a residual mean greater than zero, and the IMW (Figure 3c) and V1 (Figure 3d) models had residual means less than zero (Table 5), revealing that they tended to overestimate and  
450 underestimate postfire debris-flow volumes in this dataset, respectively. The WEST model also had the lowest standard deviation ( $\sigma$ ) of all four models (Table 6), indicating the variability of the residuals was lower compared to the other three models. Finally, the WEST model had the lowest MAE (Table 7) and predicted the greatest percentage of volumes within an order of magnitude (Table 8), further indicating that it provided the best fit between modeled and observed volumes in the western United States.

**Table 5:** Residual means for the western US (WEST), Emergency Assessment volume (EAV), Intermountain West (IMW), and V1 models (subset by region)

<b>Model</b>	<b>Residual Mean (<math>\mu</math>)</b>				
	<b>Western United States</b>	<b>Southern California</b>	<b>Intermountain West</b>	<b>Southwest</b>	<b>Data-Limited Regions</b>
WEST	-0.003	-0.70	0.42	0.41	0.75
EAV	1.32	-0.01	2.31	2.52	2.14
IMW	-2.91	-3.83	-2.61	-2.96	-0.07
V1	-2.02	-3.26	-1.12	-0.50	-1.51

455

The WEST model also performed well relative to existing models, when evaluated against subsets of data from regions where the other volume models were developed, including southern California (Figure S2), the Intermountain West (Figure S4), and the Southwest (Figure S5). In southern California, the WEST model was the second best-performing model, just behind the EAV model, which was developed for use in this region. Although the EAV model had a lower  
460 MAE (Table 7) and a predicted a higher percentage of volumes within an order of magnitude (Table 8), the difference in performance between the EAV and WEST models was marginal, especially when compared to the IMW and V1 models (Figure S2). The IMW and V1 models both had MAE values nearly double that of the EAV and WEST models (Table 7) and predicted less than 20% of southern California volumes within an order of magnitude (Table 8). Both models also tended to substantially underpredict debris-flow volumes in southern California, whereas the WEST  
465 model only slightly underpredicted volumes in this region, on average (Table 5). The EAV model neither systemically overpredicted nor underpredicted volumes in southern California, as evidenced by a residual mean value of -0.01 (Table 5).

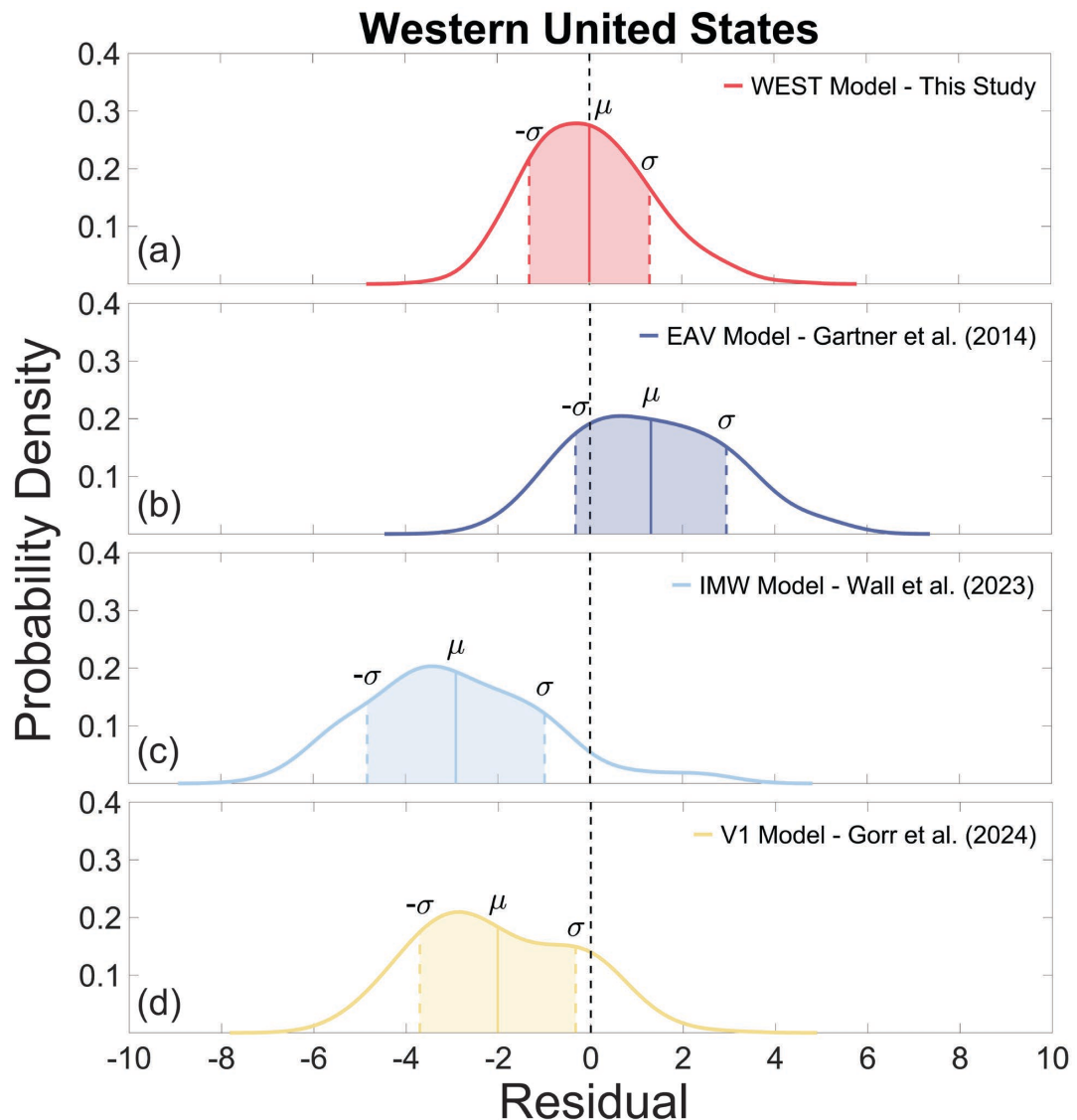


Figure 3: Probability density functions for the residuals of the (a) western United States (WEST), (b) Emergency Assessment volume (EAV), (c) Intermountain West (IMW), and (d) V1 models when applied to the entire western United States dataset.



**Table 6:** Standard deviation of the residuals for the western US (WEST), Emergency Assessment volume (EAV), Intermountain West (IMW), and V1 models (subset by region)

Model	Standard Deviation ( $\sigma$ )				
	Western	Southern	Intermountain	Southwest	Data-Limited Regions
	United States	California	West		
WEST	1.30	1.07	1.20	1.22	1.37
EAV	1.63	0.95	1.31	1.24	1.29
IMW	1.92	1.52	1.62	1.63	1.99
V1	1.69	0.96	1.54	1.25	1.47

475

**Table 7:** Median absolute errors for the western US (WEST), Emergency Assessment volume (EAV), Intermountain West (IMW), and V1 models (subset by region)

Model	Median Absolute Error (m <sup>3</sup> )				
	Western	Southern	Intermountain	Southwest	Data-Limited Regions
	United States	California	West		
WEST	1,581	5,037	794	753	269
EAV	7,088	4,407	10,070	10,717	2,495
IMW	2,256	9,627	1,165	1,097	411
V1	1,738	9,160	664	594	245

**Table 8:** Percentage of volumes predicted within an order of magnitude by the western US (WEST), Emergency Assessment volume (EAV), Intermountain West (IMW), and V1 models (subset by region)

Model	Percentage of Volumes Predicted within an Order of Magnitude				
	Western	Southern	Intermountain	Southwest	Data-Limited Regions
	United States	California	West		
WEST	93%	96%	93%	93%	84%
EAV	67%	98%	44%	34%	63%
IMW	35%	18%	45%	38%	58%
V1	52%	17%	76%	90%	74%

In some scenarios, the WEST model even outperformed existing models in the regions for which they were developed, including the Intermountain West (Figure S4) and the Southwest (Figure S5). In the Intermountain West, the WEST model outperformed the IMW model (Figure S4). It had a lower MAE (Table 7) than the IMW model and predicted a

480



greater percentage of volumes within an order of magnitude (Table 8) in this region. Furthermore, the residual mean of the WEST model was closer to zero (Table 5) and its standard deviation was smaller than that of the IMW model (Table 6), which systemically underpredicted volumes in the Intermountain West (Figure S4). The WEST model also outperformed both the EAV and V1 models in the Intermountain West, as the EAV model greatly overpredicted debris-flow volume, on average, and the V1 model underpredicted debris-flow volume, on average (Figure S4). In the Southwest, the WEST model outperformed the V1 model, according to most metrics (Figure S5). Although the V1 model had a slightly lower MAE (Table 7), the WEST model predicted a greater percentage of volumes in the Southwest within an order of magnitude (Table 8), had a smaller standard deviation (Table 6), and had a residual mean closer to zero (Table 5). The WEST model tended to slightly overpredict debris-flow volumes in the Southwest (Figure S5), whereas the V1 model tended to slightly underpredict volumes in this region (Figure S5d). The EAV and IMW models, on the other hand, more severely overpredicted and underpredicted volumes in the Southwest, respectively (Figure S5). Differences between the volumes predicted by these models and observed volumes in the Southwest routinely exceeded an order of magnitude (Table 8).

When applied to 19 postfire debris-flow volumes from data-limited regions, including northern California, Utah, and Washington, (Table S2), the WEST model again outperformed the EAV, IMW, and V1 models. The WEST model predicted the greatest percentage of volumes within an order of magnitude (Figure 4; Table 8) and had one of the lowest MAE values (Table 7). Although the IMW model had the residual mean closest to zero (Table 5), it also had the largest standard deviation (Table 6), indicating high variability in the residuals compared to other models (Figure 5). The WEST model slightly overpredicted volumes from data-limited regions but had the lowest standard deviation of the four models (Table 6). The EAV model overpredicted volumes from data-limited regions more substantially (Figure 5b), whereas the V1 model underpredicted volumes from data-limited regions, on average (Figure 5d).



## Data-Limited Regions

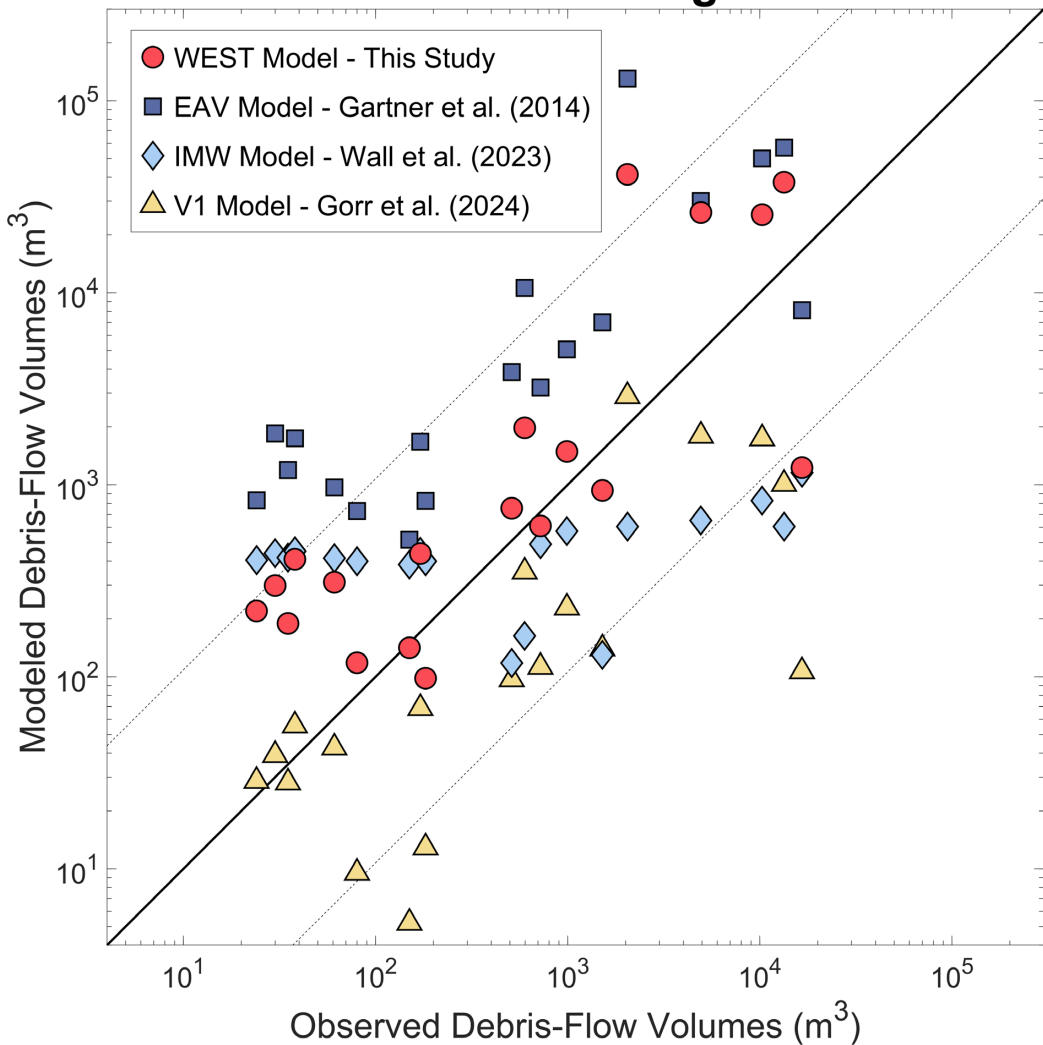
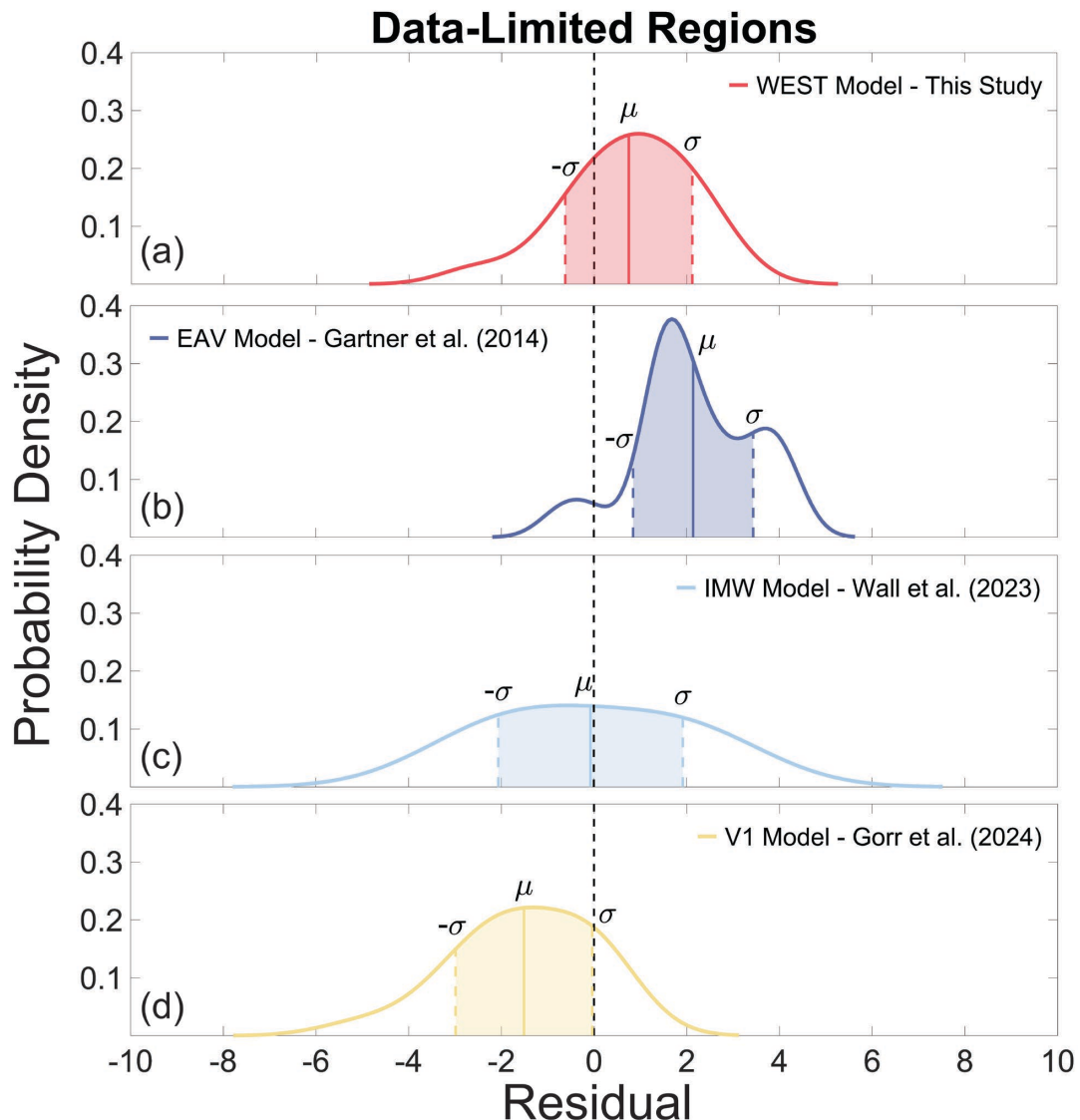


Figure 4: A comparison between the observed volume of 19 postfire debris flows from data-limited regions and the corresponding volume predicted by the western United States (WEST), Emergency Assessment volume (EAV), Intermountain West (IMW), and V1 models. The thick, black line is a 1:1 line, and the thin, dashed lines represent an order of magnitude envelope.

505



510 **Figure 5: Probability density functions for the residuals of the (a) western United States (WEST), (b)  
Emergency Assessment volume (EAV), (c) Intermountain West (IMW), and (d) V1 models when applied to  
volumes from data-limited regions.**

## 5 Discussion

In this study, we introduced a new empirical model for predicting postfire debris-flow volume in the western United States. This model, referred to as the WEST model, predicts the volume of sediment deposited by postfire debris flows as a function of  $i30$  rainfall ratio, watershed area, and watershed area burned at moderate or high severity with slopes



greater than or equal to 50% (Eq. 2). It offers an improvement over existing volume models because it accounts for regional differences in rainfall characteristics with a rainfall ratio metric and because it was trained on a larger dataset of debris-flow volumes from across the western United States. Specifically, the WEST model outperforms three 520 existing debris-flow volume models (Gartner et al., 2014; Wall et al., 2023; Gorr et al., 2024a) when applied to the entire western United States database (Figure 3), as well as to subsets of data from the Intermountain West (Figure S4), the Southwest (Figure S5), and data-limited regions (Figures 4 and 5). It also maintains a similar level of performance to that of a model developed for use in southern California when applied in that region (Figure S2). These results indicate that the WEST model is more broadly applicable than existing volume models, particularly in data-limited regions, and that it may be a promising tool for postfire hazard assessment in the western United States. 525

### 5.1 Improvements over existing models

#### 5.1.1 Rainfall ratio

The WEST model offers an improvement over existing volume models because it accounts for regional differences in rainfall intensity and because it was trained on the largest dataset of debris-flow volumes. The WEST model uses a 530 rainfall ratio metric that normalizes for regional variations in rainfall and is consequently able to achieve equivalent performance to several models developed for different regions of the western United States using a single regression equation. Prior regional volume models, on the other hand, use rainfall intensity (e.g., Gartner et al., 2008, 2014; Gorr et al., 2024a), and are thus limited when applied to areas outside of their training datasets due to regional differences in the intensity of debris-flow-generating rainfall (e.g., Gorr et al., 2023, 2024a; Rengers et al., 2023, 2024). Previous 535 studies have found that, although hourly (Pak and Lee, 2008) or sub-hourly (e.g., Gartner et al., 2014; Gorr et al., 2024a) rainfall intensity is an important control on postfire debris-flow volume across the western United States, the rainfall intensity needed to generate postfire debris flows varies between regions (Cavagnaro et al., 2025b). For example, the 15-minute rainfall intensity ( $i_{15}$ ) needed to generate a postfire debris flow is less than 20 mm/h in the Transverse Ranges of southern California (Staley et al., 2013), roughly 30 mm/h in the Front Range of Colorado 540 (Staley et al., 2015), and more than 60 mm/h in northern Arizona (Youberg, 2014).

Regional volume models tend to be biased when applied outside of their training regions such that they overpredict 545 volumes in areas with higher average rainfall intensities than their training region, and underpredict volumes in areas with lower average rainfall intensities. For instance, southern California requires some of the least intense rainfall to generate postfire debris flows (Staley et al., 2017), so the EAV model (Gartner et al., 2014), which was developed using data from southern California (Gartner et al., 2014), tends to overpredict debris-flow volume in other regions of the western United States and Canada. Gorr et al. (2024a) found that the EAV model overpredicted postfire debris-flow volumes in the Southwest by roughly 3,500%, on average, and Rengers et al. (2024) found that the model overpredicted observed volumes in Colorado by more than a factor of four. Additionally, Gartner et al., (2024) found that the EAV model overpredicted postfire debris-flow volumes in British Columbia, Canada by a factor of 2 to 4. We 550 observed similar model behavior in this study, as the EAV model consistently overpredicted postfire debris-flow volume in all regions other than southern California (Figures 3, S4, and S5). Conversely, the Southwest requires some of the most intense rainfall to generate postfire debris flows (Staley et al., 2017), so the V1 model consistently overpredicted postfire debris-flow volume in the Southwest.



underpredicts postfire debris-flow volumes in other parts of the western United States (Figures 3, S3, and S4). In this  
555 study, the V1 model underestimated debris-flow volumes on all four subsets of data, as well as when applied to the  
entire western United States database (Figure 3). It performed particularly poorly when applied to southern California  
(Figure S3), the region with the least similar rainfall characteristics to the Southwest. The IMW model also consistently  
underpredicted postfire debris-flow volume in this study, including in the Intermountain West, the region for which it  
was developed (Figure S4). However, this model does not include a rainfall variable (Wall et al., 2023), indicating that  
other regional differences or model limitations are responsible for reduced performance against this volume dataset.  
560 The WEST model, however, does not exhibit large variations in model performance between geographic regions  
(Figures S3-S5) because it uses  $i30$  rainfall ratio instead of rainfall intensity (Eq. 2). This allows the WEST model to  
incorporate regional differences in rainfall intensity without the limitations associated with regional volume models.  
Because the  $i30$  rainfall ratio normalizes the peak 30-minute rainfall intensity of a debris-flow-producing storm by the  
peak 30-minute rainfall intensity associated with a 1-year recurrence interval storm at the location of a debris-flow-  
565 producing watershed, it is consistent across regions that have different rainfall characteristics. As a result, the WEST  
model performs similarly when applied to different geographic regions, including southern California (Figure S3), the  
Intermountain West (Figure S4), and the Southwest (Figure S5).

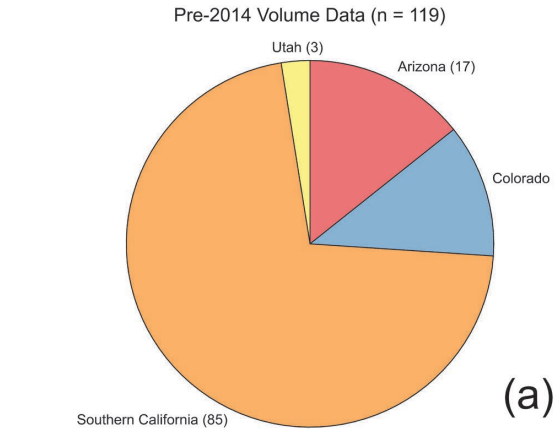
### 5.1.2 Training dataset

The WEST model also offers an improvement over existing postfire debris-flow volume models, as it was developed  
570 using a more robust training dataset. The WEST model was developed using a dataset of 227 postfire debris-flow  
volumes from 34 burn areas across six states (Figure 1). The three regional models evaluated in this study, on the other  
hand, were developed using smaller, more geographically limited datasets. Specifically, the EAV model was developed  
using 92 volumes from southern California (Gartner et al., 2014), the IMW model using 47 volumes from four states  
575 in the Intermountain West (Arizona, Colorado, Utah, and Wyoming), although 39 volumes were from Utah alone (Wall  
et al., 2023), and the V1 model using 54 volumes from Arizona and New Mexico (Gorr et al., 2024a). The geographic  
diversity of its training dataset contributes to the broader applicability of the WEST model relative to existing regional  
volume models.

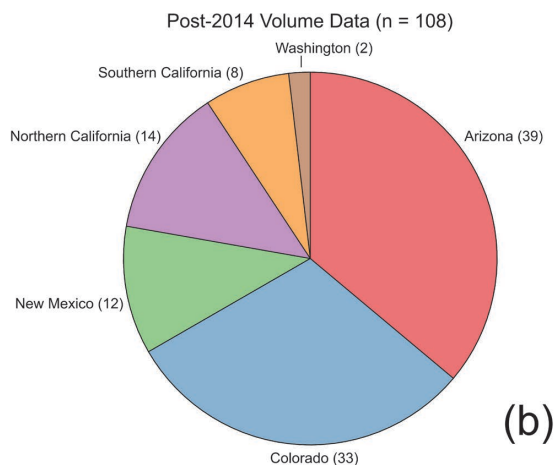
The broad applicability of the WEST model indicates that it can be a substantial improvement over volume models  
that are currently used for postfire hazard assessments, including the EAV model. The EAV model is currently the  
580 most-commonly used method for predicting postfire debris-flow volume in the western United States, as it is used as  
part of the USGS operational postfire hazard assessment framework (Landslide Hazards Program, 2018). Although  
the accuracy of the EAV model is limited outside of southern California, as discussed above, a lack of postfire debris-  
flow volume data, and associated rainfall data, in many parts of the western United States has historically prevented  
the development of a viable alternative. When the EAV model was published in 2014, nearly all measured postfire  
585 debris-flow volumes with associated rainfall data were from southern California (Gartner et al., 2014), with minor  
exceptions from Arizona (Youberg, 2014), Colorado (Gartner et al., 2008), and Utah (Gartner et al., 2008). Taking the  
database used in this study (Gorr et al., 2025) as an example, more than 70% of postfire debris-flow volumes measured



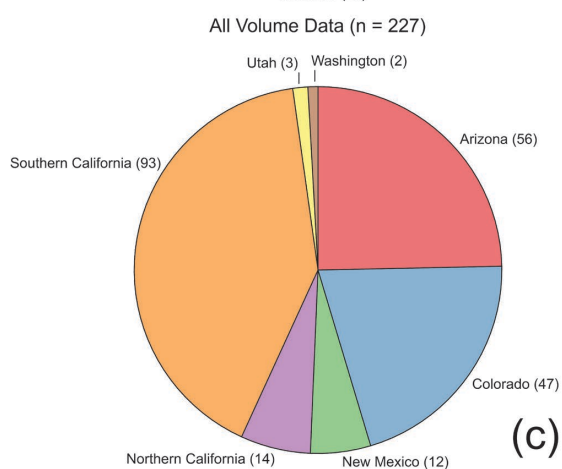
prior to 2014 came from southern California (Figure 6a). The limited geographic scope of volume data available at the time therefore prevented the development of a more broadly applicable postfire debris-flow volume model.



(a)



(b)



(c)



**Figure 6: Geographic distributions of the volume data used to develop the western United States (WEST) model, separated by date of occurrence. (a) The proportion of volume data by state collected prior to 2014. (b) The proportion of volume data by state collected in 2014 or later. (c) The proportion of data by state used in the development of the WEST model.**

595 However, efforts to measure postfire debris-flow volumes across the western United States have expanded since the EAV model was published. Of the 227 postfire debris-flow volumes used to develop the WEST model, 108 (48%) have been measured since 2014. Many of the volumes collected during this time are from regions where volume data have been historically sparse, and only 7% of post-2014 volumes used in this study are from southern California (Figure 6b). All volumes from New Mexico, northern California, and Washington have been collected since 2014, and  
600 data from Arizona and Colorado have expanded by 229% and 236% relative to the pre-2014 dataset, respectively (Figure 6c). The improved performance of the WEST model across the western United States compared to existing models can therefore be partially attributed to the fact that it was trained on the largest and most geographically diverse postfire debris-flow volume dataset with associated rainfall data.

## 5.2 Implications for hazard assessment

605 Because it accounts for regional differences in rainfall characteristics and was trained on a geographically diverse volume dataset, the WEST model can be used for widespread postfire hazard assessments in the western United States. One of the most encouraging signs for improved postfire hazard assessments is the model's performance in data-limited regions. Results show that the WEST model performed similarly in data-limited regions as it did elsewhere in the western United States (Tables 5-8), and that it outperformed the EAV, IMW, and V1 models in these areas (Figures 610 4 and 5). The WEST model performed particularly well, relative to existing models, against two debris-flow volumes from the Dixie Fire, which burned in the Sierra Nevada of northern California, and two volumes from the Cub Creek 2 Fire, which burned in the Pacific Northwest (Washington) (Figure 1; Table 1).

615 The WEST model overpredicted the four volumes in the Sierra Nevada and Pacific Northwest by an average of 25,007 m<sup>3</sup>, which represents a substantial improvement over the EAV model, which overpredicted the same four volumes by an average of 59,284 m<sup>3</sup>. The IMW and V1 models, on the other hand, underpredicted these volumes by an average of 6,981 m<sup>3</sup> and 5,792 m<sup>3</sup>, respectively. Though the IMW and V1 models provided a smaller absolute difference between observed and modeled volumes in these regions, they severely underpredicted observed volumes in the Sierra Nevada and Pacific Northwest. Specifically, the IMW model underpredicted these four volumes by between 70.5% and 95.5%. The V1 model slightly overpredicted one of the four volumes by 41%, but underpredicted the remaining three by between 63.5% and 92.4%. Because previous studies have found that debris-flow volume scales with runoff distance and area inundated (Iverson et al., 1998; Rickenmann, 1999; Griswold and Iverson, 2008), underpredicting debris-flow volume limits the effectiveness of postfire hazard assessments by underestimating the downstream effects of postfire debris flows. Based on the results of this study, the WEST model is less likely to underestimate the extent of potential downstream effects from postfire debris flows in data-limited regions, as it offers more conservative predictions of postfire debris-flow volume relative to the IMW and V1 models. At the same time, it provides more  
620  
625



accurate volume estimates than the EAV model in these areas, making it less likely to predict unrealistically severe downstream effects.

Having a method that outperforms existing models in data-limited regions, such as the Sierra Nevada and Pacific Northwest, can improve postfire hazard assessments in these areas, particularly as fire activity increases. Wildfire activity across the western United States has increased considerably in recent decades, but this change has been particularly pronounced in the Pacific Northwest (Westerling, 2016). According to Westerling (2016), the area burned by wildfire in the Pacific Northwest between 2003 and 2012 increased by nearly 5,000% relative to the area burned in this region between 1973 and 1982. Furthermore, since this study was published in 2016, the Pacific Northwest has experienced multiple historic fire seasons, including the 2020 season, which burned nearly as much forest in the western Cascade Range in two weeks as the previous five decades combined (Reilly et al., 2022). Fire activity is also increasing in California's Sierra Nevada (Westerling, 2016). Not only are fires in the Sierra Nevada increasing in size and frequency (Westerling, 2016), but the severity of fires is also changing. Miller and Safford (2012) found that proportion of annual wildfire burned at high severity increased considerably in parts of the Sierra Nevada between 1984 and 2010. This has important implications for postfire debris-flow hazards, as the effects of fire on infiltration and erosion, which affects debris-flow initiation and growth, are most pronounced in areas burned at high severity (e.g., Vieira et al., 2015; McGuire and Youberg, 2019). As fire activity in these regions increases, so does the potential for postfire debris-flow hazards (e.g., DeGraff et al., 2011; Neptune et al., 2021; Wall et al., 2020; Selander et al., 2025), underscoring the use of a volume model, like the WEST model, that can provide accurate estimates of debris-flow volume in these areas.

Additional volume data from the Sierra Nevada and Pacific Northwest can be used to continue improving volume predictions in these regions, but this study represents a first step, as it is the first study to include data from the Sierra Nevada and Pacific Northwest in the development and evaluation of volume models. Additionally, volume data from the northern Rockies (Idaho, Montana, and Wyoming) are needed to help to evaluate the WEST model in this region. Although the northern Rockies are susceptible to postfire debris flows (e.g., Meyer and Wells, 1997; Gabet and Bookter, 2008), we are unaware of any postfire debris-flow volumes with associated rainfall data from this region that can be used to improve model performance.

### 5.3 Model limitations and future work

Although the WEST model improves our ability to predict postfire debris-flow volume in many regions of the western United States, there are some scenarios where the model's effectiveness may be limited. For example, because the WEST model predicts postfire debris-flow volume as a function of both watershed area and watershed area burned at moderate or high severity with slopes greater than or equal to 50%, it tends to substantially overpredict volumes from large watersheds ( $>20 \text{ km}^2$ ) (Figure 6). We observed this model behavior when applied to the largest watershed in the dataset used in this study: Cucamonga Dam (Gorr et al., 2025). The Cucamonga Dam watershed, which burned in the 2003 Grand Prix Fire in southern California (Figure 1), had an area of  $28.0 \text{ km}^2$  and an area burned at moderate or high severity with slopes greater than or equal to 50% of  $14.8 \text{ km}^2$ , both the largest in the volume dataset (Tables 3 and 4). It also produced the largest postfire debris flow in the dataset, with a volume of  $801,770 \text{ m}^3$  (Gorr et al., 2025).



When applied to this watershed, the WEST model predicted a volume of 1,993,100 m<sup>3</sup>, an overprediction of more than 1,000,000 m<sup>3</sup> (Figure 7). However, we only expect this behavior in the watersheds larger than 20 km<sup>2</sup>, like the Cucamonga Dam watershed, as the model slightly underpredicted the volumes for the next two largest watersheds in the dataset (Figure 7), which had areas of 17.3 km<sup>2</sup> and 14.4 km<sup>2</sup>. This limitation is unlikely to affect postfire hazard assessments in the western US, as the USGS operational postfire hazard assessment framework is typically applied to watersheds with areas less than 8.0 km<sup>2</sup> (Landslide Hazards Program, 2018).

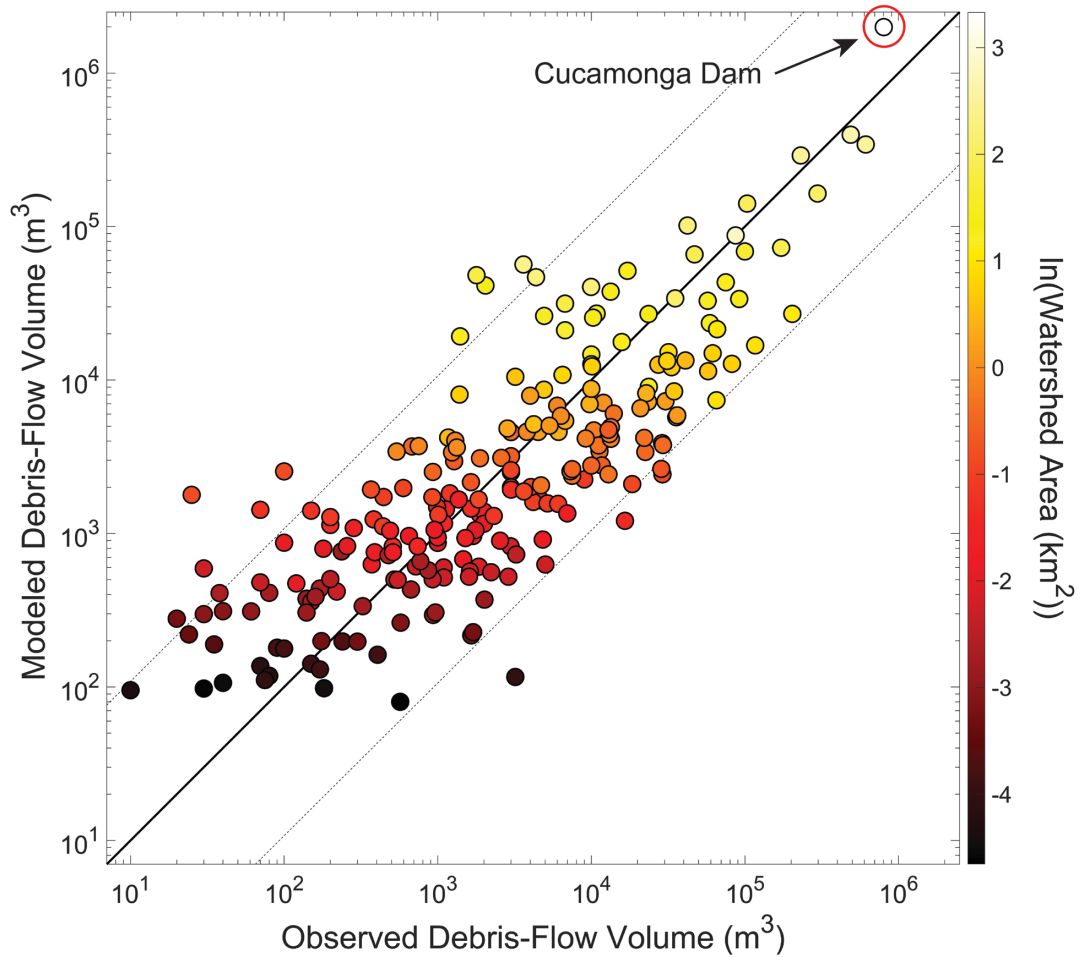


Figure 7: Comparison between observed debris-flow volumes and debris-flow volumes predicted by the Western United States (WEST) model when applied to the entire western United States dataset. Points are colored by the natural log of the area of the debris-flow-producing watershed. The thick, black line is a 1:1 line, and the thin, dashed lines represent an order of magnitude envelope.



Another potential limitation of the WEST model is that, aside from differences in rainfall characteristics, it does not account for other regional factors that may influence postfire debris-flow volume, including sediment availability. In  
675 southern California, dry ravel (i.e., the transport of sediment by gravity without rainfall) is a common process in burned landscapes (e.g., Lamb et al., 2011). Following fire, but before rainfall, dry ravel can load channels with up to three meters of unconsolidated sediment that serves as an important sediment source for postfire debris flows (e.g., Wells, 1987; DiBiase and Lamb, 2020; Palucis et al., 2021). Although prevalent in southern California, dry ravel is less common in other regions of the western United States (Perkins et al., 2022). Previous studies have found that  
680 rilling on hillslopes and/or channel incision, not dry ravel, are the primary sources of sediment for postfire debris flows in many areas, including elsewhere in California (e.g., DeGraff et al., 2011), Colorado (Rengers et al., 2024), the Pacific Northwest (Wall et al., 2020), and the Southwest (e.g., Tillery and Rengers, 2020; Gorr et al., 2024b), among others. The absence of dry ravel in these regions may limit sediment availability and result in smaller postfire debris-flow volumes relative to southern California. Regional differences in sediment availability may account for differences  
685 in model behavior that we observed in this study. In areas with dry ravel (i.e., southern California), the WEST model is biased low (Figure S3), and in areas where dry ravel is less prevalent (i.e., the Intermountain West and Southwest), the WEST model is biased high (Figures S4 and S5). This indicates that future postfire debris-flow volume models may benefit from the inclusion of a sediment availability variable.

## 6 Conclusions

690 Debris-flow volume is a critical component of postfire hazard assessments in the western United States. However, existing methods for predicting postfire debris-flow volume have various shortcomings that limit their applicability for the purpose of postfire hazard assessment. In this study, we introduced a new model for predicting postfire debris-flow volume in the western United States. Using a database of 227 postfire debris-flow volumes collected across six states and 34 burn areas, we developed a multiple linear regression model that predicts postfire debris-flow volume as  
695 a function of rainfall, watershed terrain, and fire characteristics. This model offers an improvement over existing volume models, as it accounts for regional differences in debris-flow-generating rainfall and was trained on a larger, more geographically diverse volume dataset. Results from this study demonstrate that the new model outperforms three existing regional volume models when applied to the entire western United States database, and either outperforms or performs similarly to existing regional volume models when applied to subsets of volume data from  
700 the regions for which they were developed. The new model also outperforms existing models when applied to volumes from data-limited regions where there is not enough data to develop region-specific models. The broad applicability of the model introduced in this study indicates that it can be used to improve widespread postfire hazard assessments across the western United States.

## Data availability

705 The data used to develop the WEST model are publicly available in Gorr et al. (2025).

## Author contributions



ANG, FKR, KRB, MAT, and JWK conceptualized the study. ANG and FKR collected data with assistance from co-authors. ANG performed data analysis with assistance from all co-authors. ANG prepared the original draft of the manuscript, and FKR, KRB, MAT, and JWK reviewed and edited the draft.

710 **Competing Interests**

The authors declare that they have no conflict of interest.

**Acknowledgements**

We thank Joseph Gartner (BGC Engineering) and Jacob Woodard (U.S. Geological Survey) for their work reviewing this paper. We also thank those who contributed new volume data, beyond what has already been reported in previous 715 studies, including Corey Crowder and Luke McGuire (University of Arizona), Andrew Gruber, Olivia Hoch, and Jaime Kostelnik (U.S. Geological Survey), and Don Lindsay and Paul Richardson (California Geological Survey). Any use of trade, firm, or product names is for descriptive purposes only and does not imply endorsement by the U.S. Government.

**References**

720 Alin, A.: Multicollinearity, *WIREs Computational Statistics*, 2, 370–374, <https://doi.org/10.1002/wics.84>, 2010.

Anderson, T. W. and Darling, D. A.: A Test of Goodness of Fit, *Journal of the American Statistical Association*, 49, 765–769, <https://doi.org/10.1080/01621459.1954.10501232>, 1954.

Barnhart, K. R., Jones, R. P., George, D. L., McArdell, B. W., Rengers, F. K., Staley, D. M., and Kean, J. W.: Multi-Model Comparison of Computed Debris Flow Runout for the 9 January 2018 Montecito, California Post-Wildfire 725 Event, *Journal of Geophysical Research: Earth Surface*, 126, e2021JF006245, <https://doi.org/10.1029/2021JF006245>, 2021.

Berti, M. and Simoni, A.: Prediction of debris flow inundation areas using empirical mobility relationships, *Geomorphology*, 90, 144–161, <https://doi.org/10.1016/j.geomorph.2007.01.014>, 2007.

Bonnin, G. M., Martin, D., Lin, B., Parzybok, T., Yekta, M., and Riley, D.: Precipitation-Frequency Atlas of the United 730 States. Volume 1, Version 5.0. Semiarid Southwest (Arizona, Southeast California, Nevada, New Mexico, Utah), 2006.

Brown, M. B. and Forsythe, A. B.: Robust Tests for the Equality of Variances, *Journal of the American Statistical Association*, 69, 364–367, <https://doi.org/10.1080/01621459.1974.10482955>, 1974.

Cannon, S., Gartner, J., Rupert, M., Michael, J., Rea, A., and Parrett, C.: Predicting the probability and volume of postwildfire debris flows in the intermountain western United States, *Geological Society of America Bulletin*, 122, 735 127–144, <https://doi.org/10.1130/B26459.1>, 2010.

Cannon, S. H., Kirkham, R. M., and Parise, M.: Wildfire-related debris-flow initiation processes, *Storm King Mountain, Colorado*, *Geomorphology*, 39, 171–188, [https://doi.org/10.1016/S0169-555X\(00\)00108-2](https://doi.org/10.1016/S0169-555X(00)00108-2), 2001.



740 Cannon, S. H., Gartner, J. E., Wilson, R. C., Bowers, J. C., and Laber, J. L.: Storm rainfall conditions for floods and debris flows from recently burned areas in southwestern Colorado and southern California, *Geomorphology*, 96, 250–269, <https://doi.org/10.1016/j.geomorph.2007.03.019>, 2008.

745 Cannon, S. H. and Gartner, J. E.: Wildfire-related debris flow from a hazards perspective, in: *Debris-flow Hazards and Related Phenomena*, edited by: Jakob, M. and Hungr, O., Springer, Berlin, Heidelberg, 363–385, [https://doi.org/10.1007/3-540-27129-5\\_15](https://doi.org/10.1007/3-540-27129-5_15), 2005.

750 Cavagnaro, D. B., McCoy, S. W., Thomas, M. A., Kostelnik, J., and Lindsay, D. N.: Improved Prediction of Postfire Debris Flows Through Rainfall Anomaly Maps, *Geophysical Research Letters*, 52, e2025GL114791, <https://doi.org/10.1029/2025GL114791>, 2025a.

Cavagnaro, D. B., McCoy, S. W., Lindsay, D. N., McGuire, L. A., Kean, J. W., and Trugman, D. T.: Rainfall Thresholds for Postfire Debris-Flow Initiation Vary With Short-Duration Rainfall Climatology, *Journal of Geophysical Research: Earth Surface*, 130, e2024JF007781, <https://doi.org/10.1029/2024JF007781>, 2025b.

755 Daurio, M.: Cascading hazards, cascading consequences: Linking social-ecological systems in post-fire recovery, *Human Organization*, 84, 339–350, <https://doi.org/10.1080/00187259.2025.2499680>, 2025.

DeGraff, J. V., Wagner, D. L., Gallegos, A. J., DeRose, M., Shannon, C., and Ellsworth, T.: The remarkable occurrence of large rainfall-induced debris flows at two different locations on July 12, 2008, Southern Sierra Nevada, CA, USA, *Landslides*, 8, 343–353, <https://doi.org/10.1007/s10346-010-0245-5>, 2011.

760 DiBiase, R. A. and Lamb, M. P.: Dry sediment loading of headwater channels fuels post-wildfire debris flows in bedrock landscapes, *Geology*, 48, 189–193, <https://doi.org/10.1130/G46847.1>, 2020.

Donovan, I. P. and Santi, P. M.: A probabilistic approach to post-wildfire debris-flow volume modeling, *Landslides*, 14, 1345–1360, <https://doi.org/10.1007/s10346-016-0786-3>, 2017.

Dowling, C. A. and Santi, P. M.: Debris flows and their toll on human life: a global analysis of debris-flow fatalities from 1950 to 2011, *Nat Hazards*, 71, 203–227, <https://doi.org/10.1007/s11069-013-0907-4>, 2014.

765 Drummond, M. A.: Southern Rockies Ecoregion, in *Status and Trends of Land Change in the Western United States – 1973 to 2000*, edited by: Sleeter B. M., Wilson, T. S., and Acevedo, W., U.S. Geological Survey, 95-103, <https://pubs.usgs.gov/pp/1794/a/>, 2012.

Gabet, E. J. and Bookter, A.: A morphometric analysis of gullies scoured by post-fire progressively bulked debris flows in southwest Montana, USA, *Geomorphology*, 96, 298–309, <https://doi.org/10.1016/j.geomorph.2007.03.016>, 2008.

Gartner, J. E., Cannon, S. H., Santi, P. M., and Dewolfe, V. G.: Empirical models to predict the volumes of debris flows generated by recently burned basins in the western U.S., *Geomorphology*, 96, 339–354, <https://doi.org/10.1016/j.geomorph.2007.02.033>, 2008.



770 Gartner, J. E., Cannon, S. H., and Santi, P. M.: Empirical models for predicting volumes of sediment deposited by debris flows and sediment-laden floods in the transverse ranges of southern California, *Engineering Geology*, 176, 45–56, <https://doi.org/10.1016/j.enggeo.2014.04.008>, 2014.

775 Gartner, J. E., Kean, J. W., Rengers, F. K., McCoy, S. W., Oakley, N., and Sheridan, G.: Post-Wildfire Debris Flows, in: *Advances in Debris-flow Science and Practice*, edited by: Jakob, M., McDougall, S., and Santi, P., Springer International Publishing, Cham, 309–345, [https://doi.org/10.1007/978-3-031-48691-3\\_11](https://doi.org/10.1007/978-3-031-48691-3_11), 2024.

Gorr, A.N., Rengers, F.K., Barnhart, K.R., Thomas, M.A., Kean, J.W., and Crowder, C.A.: Inventory of 227 postfire debris-flow volumes for 34 fires in the western United States, United States Geological Survey Data Release, <https://doi.org/10.5066/P13EZSWW>, 2025.

780 Gorr, A. N., McGuire, L. A., and Youberg, A. M.: Empirical Models for Postfire Debris-Flow Volume in the Southwest United States, *Journal of Geophysical Research: Earth Surface*, 129, e2024JF007825, <https://doi.org/10.1029/2024JF007825>, 2024a.

Gorr, A. N., McGuire, L. A., Youberg, A. M., Beers, R., and Liu, T.: Inundation and flow properties of a runoff-generated debris flow following successive high-severity wildfires in northern Arizona, USA, *Earth Surface Processes and Landforms*, 49, 622–641, <https://doi.org/10.1002/esp.5724>, 2024b.

785 Gorr, A. N., McGuire, L. A., Youberg, A. M., and Rengers, F. K.: A progressive flow-routing model for rapid assessment of debris-flow inundation, *Landslides*, 19, 2055–2073, <https://doi.org/10.1007/s10346-022-01890-y>, 2022.

Gorr, A. N., McGuire, L. A., Beers, R., and Hoch, O. J.: Triggering conditions, runout, and downstream impacts of debris flows following the 2021 Flag Fire, Arizona, USA, *Nat Hazards*, 117, 2473–2504, <https://doi.org/10.1007/s11069-023-05952-9>, 2023.

790 Griffith, G. E., Omernik, J. M., Smith, D. W., Cook, T. D., Tallyn, E., Moseley, K., and Johnson, C. B.: Ecoregions of California, U.S. Geological Survey, Open-File Report 2016-1021, <https://doi.org/10.3133/ofr20161021>, 2016.

Griswold, J. P. and Iverson, R. M.: Mobility statistics and automated hazard mapping for debris flows and rock avalanches, *Scientific Investigations Report*, U.S. Geological Survey, <https://doi.org/10.3133/sir20075276>, 2008.

795 Guthrie, R. H., Friele, P., Allstadt, K., Roberts, N., Evans, S. G., Delaney, K. B., Roche, D., Clague, J. J., and Jakob, M.: The 6 August 2010 Mount Meager rock slide-debris flow, Coast Mountains, British Columbia: characteristics, dynamics, and implications for hazard and risk assessment, *Natural Hazards and Earth System Sciences*, 12, 1277–1294, <https://doi.org/10.5194/nhess-12-1277-2012>, 2012.

Helsel, D. R., Hirsch, R. M., Ryberg, K. R., Archfield, A., and Gilroy, E. J.: Statistical Methods in Water Resources, in: U.S. Geological Survey Techniques and Methods, <https://doi.org/10.3133/tm4A3>, 2020.



800 Hoch, O. J., McGuire, L. A., Youberg, A. M., and Rengers, F. K.: Hydrogeomorphic Recovery and Temporal Changes in Rainfall Thresholds for Debris Flows Following Wildfire, *Journal of Geophysical Research: Earth Surface*, 126, e2021JF006374, <https://doi.org/10.1029/2021JF006374>, 2021.

Iverson, R. M., Schilling, S. P., and Vallance, J. W.: Objective delineation of lahar-inundation hazard zones, *GSA Bulletin*, 110, 972–984, [https://doi.org/10.1130/0016-7606\(1998\)110<0972:ODOLIH>2.3.CO;2](https://doi.org/10.1130/0016-7606(1998)110<0972:ODOLIH>2.3.CO;2), 1998.

805 Kean, J. W., Staley, D. M., Lancaster, J. T., Rengers, F. K., Swanson, B. J., Coe, J. A., Hernandez, J. L., Sigman, A. J., Allstadt, K. E., and Lindsay, D. N.: Inundation, flow dynamics, and damage in the 9 January 2018 Montecito debris-flow event, California, USA: Opportunities and challenges for post-wildfire risk assessment, *Geosphere*, 15, 1140–1163, <https://doi.org/10.1130/GES02048.1>, 2019.

Kohavi, R.: A study of cross-validation and bootstrap for accuracy estimation and model selection, in: *Proceedings of the 14th international joint conference on Artificial intelligence - Volume 2*, San Francisco, CA, USA, 1137–1143, 1995.

810 Lamb, M. P., Scheingross, J. S., Amidon, W. H., Swanson, E., and Limaye, A.: A model for fire-induced sediment yield by dry ravel in steep landscapes, *Journal of Geophysical Research: Earth Surface*, 116, <https://doi.org/10.1029/2010JF001878>, 2011.

815 Lancaster, J. T., Swanson, B. J., Lukashov, S. G., Oakley, N. S., Lee, J. B., Spangler, E. R., Hernandez, J. L., Olson, B. P. E., DeFrisco, M. J., Lindsay, D. N., Schwartz, Y. J., McCrea, S. E., Roffers, P. D., and Tran, C. M.: Observations and Analyses of the 9 January 2018 Debris-Flow Disaster, Santa Barbara County, California, *Environmental & Engineering Geoscience*, 27, 3–27, <https://doi.org/10.2113/EEG-D-20-00015>, 2021.

820 Landslide Hazards Program: Scientific Background, <https://www.usgs.gov/programs/landslide-hazards/science/scientific-background> (last access 19 May 2025), 2018.

Langhans, C., Smith, H. G., Chong, D. M. O., Nyman, P., Lane, P. N. J., and Sheridan, G. J.: A model for assessing water quality risk in catchments prone to wildfire, *Journal of Hydrology*, 534, 407–426, <https://doi.org/10.1016/j.jhydrol.2015.12.048>, 2016.

825 Marquardt, D. W.: Generalized Inverses, Ridge Regression, Biased Linear Estimation, and Nonlinear Estimation, *Technometrics*, 12, 591–612, <https://doi.org/10.1080/00401706.1970.10488699>, 1970.

McGuire, L. A. and Youberg, A. M.: Impacts of successive wildfire on soil hydraulic properties: Implications for debris flow hazards and system resilience, *Earth Surface Processes and Landforms*, 44, 2236–2250, <https://doi.org/10.1002/esp.4632>, 2019.

830 McGuire, L. A., Youberg, A. M., Rengers, F. K., Abramson, N. S., Ganesh, I., Gorr, A. N., Hoch, O., Johnson, J. C., Lamom, P., Prescott, A. B., Zanetell, J., and Fenerty, B.: Extreme Precipitation Across Adjacent Burned and Unburned Watersheds Reveals Impacts of Low Severity Wildfire on Debris-Flow Processes, *Journal of Geophysical Research: Earth Surface*, 126, e2020JF005997, <https://doi.org/10.1029/2020JF005997>, 2021.



McGuire, L. A., Rengers, F. K., Youberg, A. M., Gorr, A. N., Hoch, O. J., Beers, R., and Porter, R.: Characteristics of debris-flow-prone watersheds and debris-flow-triggering rainstorms following the Tadpole Fire, New Mexico, USA,  
835 Natural Hazards and Earth System Sciences, 24, 1357–1379, <https://doi.org/10.5194/nhess-24-1357-2024>, 2024a.

McGuire, L. A., Ebel, B. A., Rengers, F. K., Vieira, D. C. S., and Nyman, P.: Fire effects on geomorphic processes, Nature Reviews Earth & Environment, 5, 486–503, <https://doi.org/10.1038/s43017-024-00557-7>, 2024b.

Meyer, G. A. and Wells, S. G.: Fire-related sedimentation events on alluvial fans, Yellowstone National Park, U.S.A., Journal of Sedimentary Research, 67, 776–791, <https://doi.org/10.1306/D426863A-2B26-11D7-8648000102C1865D>,  
840 1997.

Miller, J. D. and Safford, H.: Trends in Wildfire Severity: 1984 to 2010 in the Sierra Nevada, Modoc Plateau, and Southern Cascades, California, USA, Fire Ecology, 8, 41–57, <https://doi.org/10.4996/fireecology.0803041>, 2012.

Miller, J. F., Frederick, R. H., and Tracy, R. J.: Precipitation-Frequency Atlas of the Western United States. Volume IX-Washington, 1973.

845 Monitoring Trends in Burn Severity: Direct download [data set], <https://www.mtbs.gov/direct-download>, 2025.

Neptune, C. K., Degraff, J. V., Pluhar, C. J., Lancaster, J. T., and Staley, D. M.: Rainfall Thresholds for Post-Fire Debris-Flow Generation, Western Sierra Nevada, CA, Environmental & Engineering Geoscience, 27, 439–453, <https://doi.org/10.2113/EEG-D-21-00039>, 2021.

Pak, J. H. and Lee, J. J.: A Statistical Sediment Yield Prediction Model Incorporating the Effect of Fires and  
850 Subsequent Storm Events, Journal of the American Water Resources Association, 44, 689–699, <https://doi.org/10.1111/j.1752-1688.2008.00199.x>, 2008.

Palucis, M. C., Ulizio, T. P., and Lamb, M. P.: Debris flow initiation from ravel-filled channel bed failure following wildfire in a bedrock landscape with limited sediment supply, GSA Bulletin, 133, 2079–2096, <https://doi.org/10.1130/B35822.1>, 2021.

855 Parise, M. and Cannon, S. H.: Wildfire impacts on the processes that generate debris flows in burned watersheds, Natural Hazards, 61, 217–227, <https://doi.org/10.1007/s11069-011-9769-9>, 2012.

Parsons, A., Robichaud, P. R., Lewis, S. A., Napper, C., and Clark, J. T.: Field guide for mapping post-fire soil burn severity, General Technical Report RMRS-GTR-243. Fort Collins, CO: U.S. Department of Agriculture, Forest Service, Rocky Mountain Research Station. 49 p., 2010.

860 Pelletier, J. D. and Orem, C. A.: How do sediment yields from post-wildfire debris-laden flows depend on terrain slope, soil burn severity class, and drainage basin area? Insights from airborne-LiDAR change detection, Earth Surface Processes and Landforms, 39, 1822–1832, <https://doi.org/10.1002/esp.3570>, 2014.



865 Perica, S., Dietz, S., Heim, S., Hiner, L., Maitaria, K., Martin, D., Pavlovic, S., Roy, I., Trypaluk, C., Unruh, D., Yan, F., Yekta, M., Zhao, T., Bonnin, G., Brewer, D., Chen, L.-C., Parzybok, T., and Yarchoan, J.: Precipitation-Frequency Atlas of the United States. Volume 6 Version 2.3. California, 2014.

Perica, S., Martin, D., Pavlovic, S., Roy, I., St. Laurent, M., Trypaluk, C., Unruh, D., Yekta, M., and Bonnin, G.: Precipitation-Frequency Atlas of the United States. Volume 8 Version 2.0. Midwestern States (Colorado, Iowa, Kansas, Michigan, Minnesota, Missouri, Nebraska, North Dakota, Oklahoma, South Dakota, Wisconsin), 2013.

870 Perkins, J. P., Diaz, C., Corbett, S. C., Cerovski-Darria, C., Stock, J. D., Prancevic, J. P., Micheli, E., and Jasperse, J.: Multi-Stage Soil-Hydraulic Recovery and Limited Ravel Accumulations Following the 2017 Nuns and Tubbs Wildfires in Northern California, *Journal of Geophysical Research: Earth Surface*, 127, e2022JF006591, <https://doi.org/10.1029/2022JF006591>, 2022.

875 Prescott, A. B., McGuire, L. A., Jun, K.-S., Barnhart, K. R., and Oakley, N. S.: Probabilistic assessment of postfire debris-flow inundation in response to forecast rainfall, *Natural Hazards and Earth System Sciences*, 24, 2359–2374, <https://doi.org/10.5194/nhess-24-2359-2024>, 2024.

PRISM Climate Group, Oregon State University [data set], <https://prism.oregonstate.edu>, 2025.

880 Radeloff, V. C., Helmers, D. P., Kramer, H. A., Mockrin, M. H., Alexandre, P. M., Bar-Massada, A., Butsic, V., Hawbaker, T. J., Martinuzzi, S., Syphard, A. D., and Stewart, S. I.: Rapid growth of the US wildland-urban interface raises wildfire risk, *Proceedings of the National Academy of Sciences*, 115, 3314–3319, <https://doi.org/10.1073/pnas.1718850115>, 2018.

Reilly, M. J., Zuspan, A., Halofsky, J. S., Raymond, C., McEvoy, A., Dye, A. W., Donato, D. C., Kim, J. B., Potter, B. E., Walker, N., Davis, R. J., Dunn, C. J., Bell, D. M., Gregory, M. J., Johnston, J. D., Harvey, B. J., Halofsky, J. E., and Kerns, B. K.: Cascadia Burning: The historic, but not historically unprecedented, 2020 wildfires in the Pacific Northwest, USA, *Ecosphere*, 13, e4070, <https://doi.org/10.1002/ecs2.4070>, 2022.

885 Rengers, F. K., McGuire, L. A., Barnhart, K. R., Youberg, A. M., Cadol, D., Gorr, A. N., Hoch, O. J., Beers, R., and Kean, J. W.: The influence of large woody debris on post-wildfire debris flow sediment storage, *Natural Hazards and Earth System Sciences*, 23, 2075–2088, <https://doi.org/10.5194/nhess-23-2075-2023>, 2023.

Rengers, F. K., Bower, S., Knapp, A., Kean, J. W., von Lembke, D. W., Thomas, M. A., Kostelnik, J., Barnhart, K. R., Bethel, M., Gartner, J. E., Hille, M., Staley, D. M., Anderson, J. K., Roberts, E. K., DeLong, S. B., Lane, B., Ridgway, P., and Murphy, B. P.: Evaluating post-wildfire debris-flow rainfall thresholds and volume models at the 2020 Grizzly Creek Fire in Glenwood Canyon, Colorado, USA, *Natural Hazards and Earth System Sciences*, 24, 2093–2114, <https://doi.org/10.5194/nhess-24-2093-2024>, 2024.

890 Rickenmann, D. and Zimmermann, M.: The 1987 debris flows in Switzerland: documentation and analysis, *Geomorphology*, 8, 175–189, [https://doi.org/10.1016/0169-555X\(93\)90036-2](https://doi.org/10.1016/0169-555X(93)90036-2), 1993.



895 Rickenmann, D.: Empirical Relationships for Debris Flows, *Natural Hazards*, 19, 47–77, <https://doi.org/10.1023/A:1008064220727>, 1999.

Santi, P. M. and Morandi, L.: Comparison of debris-flow volumes from burned and unburned areas, *Landslides*, 10, 757–769, <https://doi.org/10.1007/s10346-012-0354-4>, 2013.

900 Santi, P. M.: Precision and Accuracy in Debris-Flow Volume Measurement, *Environmental & Engineering Geoscience*, 20, 349–359, <https://doi.org/10.2113/gsengeosci.20.4.349>, 2014.

Selander, B. D., Calhoun, N., Burns, W. J., Kean, J. W., and Rengers, F. K.: Assessment of western Oregon debris-flow hazards in burned and unburned environments, *Earth Surface Processes and Landforms*, 50, e70045, <https://doi.org/10.1002/esp.70045>, 2025.

905 Sepúlveda, S. A., Rebolledo, S., and Vargas, G.: Recent catastrophic debris flows in Chile: Geological hazard, climatic relationships and human response, *Quaternary International*, 158, 83–95, <https://doi.org/10.1016/j.quaint.2006.05.031>, 2006.

910 Smith, D. P., Schnieders, J., Marshall, L., Melchor, K., Wolfe, S., Campbell, D., French, A., Randolph, J., Whitaker, M., Klein, J., Steinmetz, C., and Kwan, R.: Influence of a Post-dam Sediment Pulse and Post-fire Debris Flows on Steelhead Spawning Gravel in the Carmel River, California, *Front. Earth Sci.*, 9, <https://doi.org/10.3389/feart.2021.802825>, 2021.

Smith, H. G., Sheridan, G. J., Lane, P. N. J., Nyman, P., and Haydon, S.: Wildfire effects on water quality in forest catchments: A review with implications for water supply, *Journal of Hydrology*, 396, 170–192, <https://doi.org/10.1016/j.jhydrol.2010.10.043>, 2011.

915 Smith, T., Rheinwalt, A., and Bookhagen, B.: Determining the optimal grid resolution for topographic analysis on an airborne lidar dataset, *Earth Surface Dynamics*, 7, 475–489, <https://doi.org/10.5194/esurf-7-475-2019>, 2019.

Staley, D. M., Kean, J. W., Cannon, S. H., Schmidt, K. M., and Laber, J. L.: Objective definition of rainfall intensity-duration thresholds for the initiation of post-fire debris flows in southern California, *Landslides*, 10, 547–562, <https://doi.org/10.1007/s10346-012-0341-9>, 2013.

920 Staley, D. M., Gartner, J. E., and Kean, J. W.: Objective Definition of Rainfall Intensity-Duration Thresholds for Post-fire Flash Floods and Debris Flows in the Area Burned by the Waldo Canyon Fire, Colorado, USA, in: *Engineering Geology for Society and Territory - Volume 2*, Springer, Cham, 621–624, [https://doi.org/10.1007/978-3-319-09057-3\\_103](https://doi.org/10.1007/978-3-319-09057-3_103), 2015.

925 Staley, D. M., Negri, J. A., Kean, J. W., Laber, J. L., Tillery, A. C., and Youberg, A. M.: Prediction of spatially explicit rainfall intensity-duration thresholds for post-fire debris-flow generation in the western United States, *Geomorphology*, 278, 149–162, <https://doi.org/10.1016/j.geomorph.2016.10.019>, 2017.



Staley, D. M., Kean, J. W., and Rengers, F. K.: The recurrence interval of post-fire debris-flow generating rainfall in the southwestern United States, *Geomorphology*, 370, 107392, <https://doi.org/10.1016/j.geomorph.2020.107392>, 2020.

930 Swanson, B. J., Lindsay, D. N., Cato, K., DiBiase, R. A., and Neely, A. B.: Debris flows and sediment transport at Yucaipa Ridge and impacts to Oak Glen and Forest Falls area, southern California, following the 2020 El Dorado and Apple Fires, in: *From Coastal Geomorphology to Magmatism: Guides to GSA Connects 2024 Field Trips in Southern California and Beyond*, vol. 70, edited by: Van Buer, N. J. and Schwartz, J. J., Geological Society of America, [https://doi.org/10.1130/2024.0070\(03\)](https://doi.org/10.1130/2024.0070(03)), 2024.

935 Thomas, M. A., Lindsay, D. N., Cavagnaro, D. B., Kean, J. W., McCoy, S. W., and Gruber, A. P.: The Rainfall Intensity-Duration Control of Debris Flows After Wildfire, *Geophysical Research Letters*, 50, e2023GL103645, <https://doi.org/10.1029/2023GL103645>, 2023.

Tillery, A. C. and Rengers, F. K.: Controls on debris-flow initiation on burned and unburned hillslopes during an exceptional rainstorm in southern New Mexico, USA, *Earth Surface Processes and Landforms*, 45, 1051–1066, <https://doi.org/10.1002/esp.4761>, 2020.

940 U.S. Environmental Protection Agency: Level III ecoregions of the continental United States, U.S. EPA – National Health and Environmental Effects Research Laboratory, Corvallis, Oregon, <https://www.epa.gov/eco-research/level-iii-and-iv-ecoregions-continental-united-states>, 2013.

945 Vieira, D. C. S., Fernández, C., Vega, J. A., and Keizer, J. J.: Does soil burn severity affect the post-fire runoff and interrill erosion response? A review based on meta-analysis of field rainfall simulation data, *Journal of Hydrology*, 523, 452–464, <https://doi.org/10.1016/j.jhydrol.2015.01.071>, 2015.

Wall, S., Murphy, B. P., Belmont, P., and Yocom, L.: Predicting post-fire debris flow grain sizes and depositional volumes in the Intermountain West, United States, *Earth Surface Processes and Landforms*, 48, 179–197, <https://doi.org/10.1002/esp.5480>, 2023.

950 Wall, S. A., Roering, J. J., and Rengers, F. K.: Runoff-initiated post-fire debris flow Western Cascades, Oregon, *Landslides*, 17, 1649–1661, <https://doi.org/10.1007/s10346-020-01376-9>, 2020.

Wang, G., Sassa, K., and Fukuoka, H.: Downslope volume enlargement of a debris slide–debris flow in the 1999 Hiroshima, Japan, rainstorm, *Engineering Geology*, 69, 309–330, [https://doi.org/10.1016/S0013-7952\(02\)00289-2](https://doi.org/10.1016/S0013-7952(02)00289-2), 2003.

955 Wells, W. G., II: The effects of fire on the generation of debris flows in southern California, in: *Debris Flows/Avalanches: Process, Recognition, and Mitigation*, vol. 7, edited by: Costa, J. E. and Wieczorek, G. F., Geological Society of America, <https://doi.org/10.1130/REG7-p105>, 1987.



Westerling, A. L.: Increasing western US forest wildfire activity: sensitivity to changes in the timing of spring, Philosophical Transactions of the Royal Society B: Biological Sciences, 371, 20150178, <https://doi.org/10.1098/rstb.2015.0178>, 2016.

960 Wilken, E., Nava, F. N., and Griffith, G.: North America Terrestrial Ecoregions – Level III. Commission for Environmental Cooperation, 2011.

Youberg, A. M.: Prehistoric and modern debris flows in semi-arid watersheds: Implications for hazard assessments in a changing climate, 2014.